NASA CR-961

EVALUATION OF TURBULENCE CORRELATIONS IN A COAXIAL FLOW OF DISSIMILAR FLUIDS

By Antonio Montealegre, Gerard J. D'Souza, and Herbert Weinstein

Prepared under Grant No. NsG-694 by
ILLINOIS INSTITUTE OF TECHNOLOGY
Chicago, Ill.

for Lewis Research Center

NATIONAL AERONAUTICS AND SPACE ADMINISTRATION

For sale by the Clearinghouse for Federal Scientific and Technical Information
Springfield, Virginia 22151 - CFSTI price $3.00

FOREWORD

Research related to advanced nuclear rocket propulsion is described herein. This work was performed under NASA Grant NsG-694 with Mr. Maynard F. Taylor, Nuclear Systems Division, NASA Lewis Research Center as Technical Manager.

ABSTRACT

A method of measuring fluctuations in velocity by means of a hot wire anemometer system has been developed and applied in a flow field where large concentration gradients exist. The flow field chosen is a coaxial flow of two dissimilar fluids with a density ratio of 4:1. The fluid medium is air and the other fluid is Freon-12.

This system is of present interest in the development of a gaseous core nuclear rocket reactor. It also finds application in the development and use of ejectors, jet pumps, after burners, combustion chambers and plasma injection systems.

Fluctuations in velocity and density are related to the fluctuations in power loss of the hot wires. However, an application of power loss correlation to data taken from two parallel wires in coaxial flow failed to give reasonable values. The reasons for the failure of this accepted method are analyzed.

The inapplicability of applying this method to the parallel wire data led to the development of the new method based on the use of an aspirating density probe in conjunction with the parallel wires. The equations found, when applied to coaxial flow data, give values that are reasonably damped with respect to density fluctuations. Also, these correlations are found to be inapplicable in certain mean velocity ranges, i.e., at low and very high velocities.

Results of calculations of velocity, density and fluctuations in velocity and density in coaxial flow of the air-freon system are presented and discussed.

TABLE OF CONTENTS

LIST OF ILLUSTRATIONS

NOMENCLATURE

SYMBOL	
A	Constant in the hot-wire anemometer equation
α	Thermal coefficient of electrical resistivity
A_τ	Eddy viscosity coefficient
A_t	Tube cross sectional area
B	Constant in the hot-wire anemometer equation
c	Concentration
d	Diameter of wire
e	Conversion constant
k_f	Thermal conductivity
l	Length of wire
M	Momentum
P	Power input to sensor
p	Fluctuating power
P_d	Power loss in aspirator probe
r	Radius-distance from centerline
R	Wire resistance
T	Time
t	Temperature
U	Component of velocity along the flow field
V	Normal velocity past the sensor
Nu	Nusselt number
Pr	Prandtl number
Re	Reynolds number

μ	Molecular viscosity
ρ	Density
θ	Time

Subscripts

1	Component 1
2	Component 2
f	film
d	density

Superscripts

-	Time average
'	Fluctuating component

I INTRODUCTION

The study of shear flows has been carried on for many years because of their wide occurrence in nature and in machinery. In the experimental studies carried out on shear flows, measurements have been made mainly of local mean velocities. Where gradients in temperature and density were also present, it usually was the mean values of these quantities that were also measured. There also has been considerable use of the hot-wire anemometer to measure fluctuating values of the velocity when there are no gradients of density or temperature present. One investigation included temperature fluctuations along with velocity fluctuations. However, investigations including velocity and density fluctuations where gradients of both properties are present in the flow field have been conspicuously lacking in the literature.

It is the object of this work to develop a method for obtaining velocity fluctuations in a shear flow with a large density gradient, using a hot-wire anemometer system. The system chosen for the investigation is one that is of present interest for gaseous core nuclear-rocket reactors. It is shown in Figure 1.1. A low velocity, high density Freon-12 jet is surrounded by a large, high velocity, low density air stream. Measurements of the velocity fluctuations are obtained in the mixing region where gradients of both the velocity and density are high.

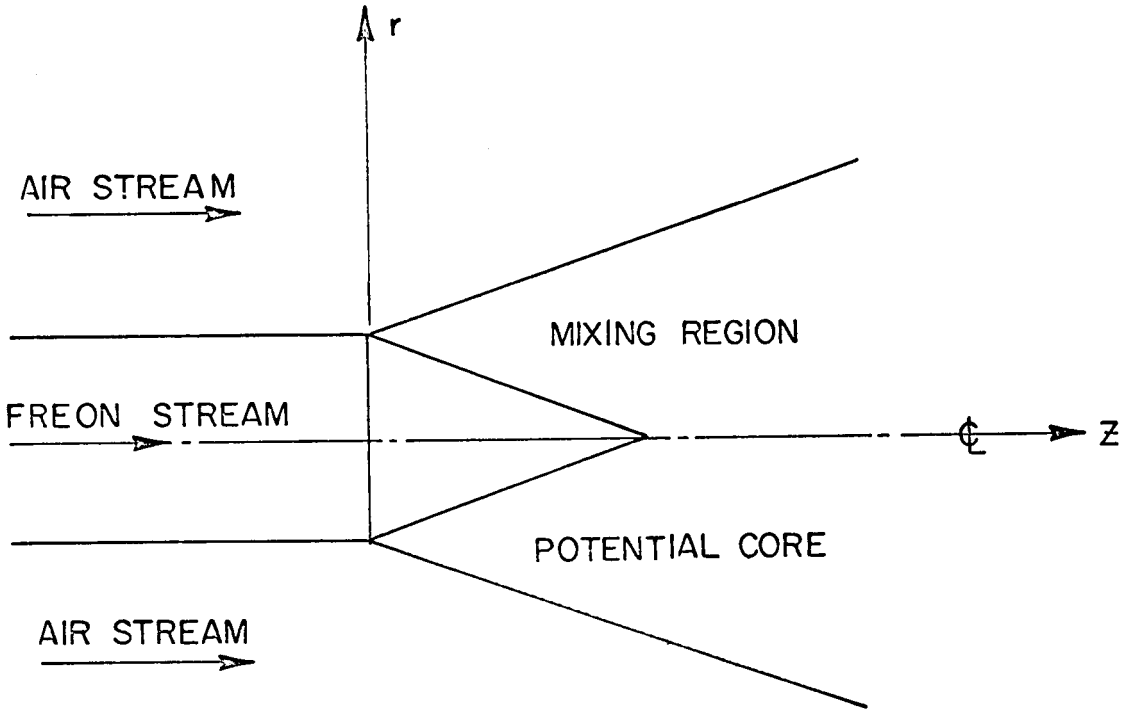

FIG. I.1 FLOW SYSTEM

Several experimental runs were made for this system which has a density ratio of 1:4 at velocity ratios ranging from 5:1 to 40:1. The data were analyzed with the method developed in this work. An attempt was also made to obtain values of the fluctuations in density, but this proved unfruitful.

II BACKGROUND

Several theoretical and experimental studies on the mixing of coaxial streams have already been made, and a brief review of these past investigations, with special reference to measurements of turbulence quantities will be presented in this chapter.

Since the flow of streams with free boundaries such as jet and coaxial flow are inherently turbulent, (except perhaps at the mouth of the flow nozzle), most of the investigations are confined to turbulent flows. These flows are characterized by a random fluctuating flow superimposed on a time smoothed flow.

$$U = \bar{U} + u' \qquad V = \bar{V} + v' \qquad \rho = \bar{\rho} + \rho' \qquad P = \bar{P} + p'$$

The average term denoted by the barred quantity is defined by taking a time average of the instantaneous component over a time interval T. This time T is large compared to the time scale of turbulence but small enough to detect slow variation or unsteadiness in the mean flow. For a general component Q, therefore,

$$\bar{Q} = \frac{1}{T} \int_{\theta}^{\theta + T} Q \, d\theta$$

and

$$\overline{q'} = \frac{1}{T} \int_{\theta}^{\theta + T} q' \, d\theta = 0$$

While the time average of any one fluctuating quantity is zero, the time average of the product of two fluctuating quantities is not necessarily zero and is zero only if the two quantities cannot be statistically related to one another.

Many of the investigations in the field of turbulent jets were involved with determining the turbulent velocity and density distribution and the value of the turbulent transport coefficient A_τ, called the eddy viscosity, from experimental techniques. A few of the investigators are: Tollmien[5], Guerther[6], Keuthe[7], Squire and Trouncer[7], Ferri et al[9], Alpinieri[10], Ragsdale et al[11], and Boehman[12]. Weinstein and Todd[13] made an analysis of the mixing of coaxial streams of dissimilar fluids and theoretically predicted the velocity and density distribution by a numerical solution of the system.

Corrsin[14] appears to be the first to report any fluctuating data on the round free jet. He measured turbulence intensities in a homogeneous jet with a hot wire anemometer and, later, with Uberoi[15], reported temperature fluctuations in a hot jet. It also appears that he was one of the first to analyze the effect of fluid stream properties on the hot wire anemometer system. In one of his reports[21] he presented the relationships between the power loss in the hot wire

and the velocity and density and that of power fluctuations to velocity fluctuations. He also mentioned the possibility of measuring density fluctuations from the power loss fluctuations of two hot wires of different diameters.

Tani and Kobashi[16] reported measurements of turbulent quantities for homogeneous coaxial flow in 1951. Their apparatus consisted of a 9 mm diameter jet exhausting into a tunnel 60 cm x 60 cm. Utilizing a hot wire anometer, they measured turbulence intensities in the axial $(\overline{u'^2})^{\frac{1}{2}}$ and radial $(\overline{v'^2})^{\frac{1}{2}}$ directions and the turbulent Reynolds stress $u'v'$. They presented curves of each quantity versus a dimensionless radius, for various axial positions, all far downstream from the jet mouth. In a continuation of the work Kobashi[17] reported temperature fluctuation measurements of a hot free jet, taken with a single wire anemometer. He reported curves of fluctuating temperature $(\overline{t'^2})^{\frac{1}{2}}$, $(\overline{u'^2})^{\frac{1}{2}}$ and the correlation $\overline{u't'}$ versus dimensionless radius.

Zawacki has also reported the turbulent terms

$$\frac{(\overline{u'^2})^{\frac{1}{2}}}{\bar{U}} \quad , \quad \frac{(\overline{v'^2})^{\frac{1}{2}}}{\bar{U}} \quad \text{and} \quad \frac{\overline{u'v'}}{(\overline{u'^2})^{\frac{1}{2}}\,(\overline{v'^2})^{\frac{1}{2}}}$$

for coaxial homogeneous constant temperature turbulent jets. His apparatus consisted of a 3/4 inch diameter jet in an 8 inch by 8 inch duct. Measurements were made using both single and cross wire hot film anemometers. He took measurements at various axial positions, close to the nozzle as well

as far downstream. Rosensweig[18] used an optical technique to measure concentration fluctuations in a smoky jet.

Blackshear and Fingerson[19] also have reported concentration fluctuation measurements in a free jet. They used a helium jet issuing from a 1.27 cm orifice into room air as a medium. Measurements were taken with an orifice or aspirator probe. These were made 15 diameters away from the orifice.

Conger[20] used a closed system wind tunnel and hot wire anemometers to measure concentration and velocity fluctuations. He assumed that because of the nature of the setup the turbulence was isotropic and, therefore, no correlation of velocity to density or temperature. Under this assumption, he could thus use a parallel wire anemometer and separate the velocity and concentration fluctuations.

III ANALYTICAL DISCUSSION

A. Fundamental Relationship

The loss of heat from small heated cylinders placed in a fluid stream was first studied extensively in connection with hot wire anemometry by King[21]. Since then, many other investigations have been undertaken. From the many experimental analyses that have been made, it is now established that the heat loss from a hot sensor can be represented by an expression of the form:

$$P = (A + BV^n)(t_s - t_e) \qquad \text{III - 1}$$

Where A and B are numerical constants, V is the normal velocity past the sensor, t_s is the temperature of the sensor, t_e is the temperature of the environment, and P the power required to maintain the sensor at the temperature t_s. The constant n is usually taken to be 1/2. An equation of this form adequately describes the power input versus velocity characteristics for hot wire anemometers so long as the velocity is sufficiently high. If the velocity is low, below about one foot per second, the power input versus square root of velocity becomes non-linear.

Experimental investigators of hot wire anemometry agree in their results, and the only difference in the analysis lies in the expression for the constants A and B. The following empirical relationship describing the heat transfer was given by Kramers[23] and is widely used.

$$Nu = 0.42\ Pr^{0.2} + 0.57\ Pr^{1/3}\ Re^{0.5} \qquad \text{III - 2}$$

Where Nu is the Nusselt number, Pr is the Prandtl number, and Re is the Reynolds number. The constants A and B are given by,

$$A = \frac{0.42\ \pi\ e\ k_f\ l\ (Pr)_f^{0.20}}{\alpha_1\ R_0} \qquad \text{III - 3}$$

$$B = \frac{0.57\ \pi\ e\ k_f\ l\ (Pr)_f^{1/3}}{\alpha_1\ R_0}\ \frac{(\rho_f\ d)^{0.5}}{\mu_f} \qquad \text{III - 4}$$

Where e is the conversion constant, k the thermal conductivity, μ the viscosity, ρ the density, α_1 the linear temperature coefficient of electrical resistivity, R_0 the wire resistance at a reference temperature t_0, l the wire length, d the wire diameter and the subscript f means the quantity is evaluated at the film temperature. The film temperature is taken as an arithmetic average of the sensor temperature, t_s, and the environment temperature t_e. Thus, the constants A and B depend on the physical properties of the surrounding medium as well as the dimensions of the wire.

In practice, A and B are experimentally determined as was done for the air and freon-air mixtures described in the report. It is also possible to calculate the equivalent length and diameter of the sensor from a pure air calibration and equations III - 3 and III - 4 and then estimate A and B

for other gas mixtures by comparing physical properties. This estimate, however, is not accurate.

B. Relationships in Concentration Measurement

The utility of hot wire anemometers lies in their response to fluid stream properties such as average concentration, average velocity and fluctuations in concentration and velocity. Thus, in non-turbulent flow of constant velocity, the density may be found by a direct application of equation III - 1 and III - 2. It may also be found through an empirical equation or graph relating density and power loss through the wire.

The density measurement is not as simple if one is measuring the density in a region of flow where both a velocity and density gradient are present. A hot film sensor mounted in a sonic aspirator probe can be used to measure concentrations in this type of flow field. Suffice it to say in this part of the discussion that the power loss from the sensor becomes a function of the molecular weight of the gas flowing past it. Hence, if P be the power input to the sensor,

$$P = P(c) \qquad \text{III - 5}$$

The above equation is valid only when there is no fluctuation in concentration. In general, if P is the average power loss and $\bar{c}$ is the average concentration, it can not be said that

$$\bar{P} = P(\bar{c}) \qquad \text{III - 6}$$

In flow streams with fluctuating concentration, the relationship of average power loss P to average concentration $\bar{c}$ may be derived as follows. The instantaneous power loss may be expressed as the sum of the mean power loss $\bar{P}$ and a fluctuating component p'. Hence,

$$P = \bar{P} + p' \qquad \text{III - 7}$$

Likewise,

$$c = \bar{c} + c' \qquad \text{III - 8}$$

Where c is instantaneous concentration at a point, $\bar{c}$ is the mean concentration at that point, and c' is the fluctuating component of concentration.

From equation III - 5, the following is obtained:

$$\bar{P} + p' = P(\bar{c} + c') \qquad \text{III - 9}$$

and by a Taylor series expansion,

$$\bar{P} + p' = P(\bar{c}) + \frac{dP}{dc} c' + \frac{d^2P}{dc^2} \frac{c'^2}{2!} + \ldots \qquad \text{III -10}$$

averaging with time,

$$\bar{P} = P(\bar{c}) + \frac{d^2P}{dc^2} \frac{\overline{c'^2}}{2!} + \frac{d^2P}{dc^3} \frac{\overline{c'^3}}{3!} + \ldots \qquad \text{III -11}$$

Thus, the average power loss in a wire does not correspond to the average concentration at a point where fluctuations exist. Equation III - 11 will be useful in a later discussion.

C. Relationships for Velocity Measurement

In non-turbulent flow, the velocity past a sensor may be calculated by a direct application of equation III - 1, assuming that the density is known. In turbulent flow, the relation between average velocity and average power loss is different from that given by equation III - 1. Two cases will be dealt with here; one applying to homogenous flow and the other to heterogenous flow.

1. Homogenous turbulent flow

The velocity V past the sensor is assumed to be made up of an average stream velocity $\bar{U}$ and fluctuating components u' and v' in the flow direction and perpendicular to the flow direction respectively. Thus,

$$V = \left[(\bar{U} + u'^2)^2 + v'^2 \right]^{\frac{1}{2}} \qquad \text{III -12}$$

The quantity V^n may be expanded in a series to give,

$$V^n = \bar{U}^n \left[1 + \frac{nu'}{\bar{U}} + \frac{n(n-1)}{2} \left(\frac{u'}{\bar{U}}\right)^2 + \frac{n}{2} \left(\frac{v'}{\bar{U}}\right)^2 + \cdots \right] \qquad \text{III -13}$$

The average power loss may be given by the equation:

$$\bar{P} = \bar{A}(c) + \overline{B(c)V^2} \qquad \text{III -14}$$

In homogenous medium

$$\bar{A}(c) = A(\bar{c}) = \text{constant}$$
$$\bar{B}(c) = B(\bar{c}) = \text{constant}$$

so that equation III - 14 becomes

$$\bar{P} = A + B\overline{V^{\frac{1}{2}}} \qquad \text{III -15}$$

Taking $n = \frac{1}{2}$ and time averaging, the following expression is obtained from equation III - 13

$$\overline{V^{\frac{1}{2}}} = \bar{U}^{\frac{1}{2}}\left[1 - \frac{1}{4}\frac{\overline{(u')^2}}{(\bar{U})} + \frac{1}{2}\frac{\overline{(v')^2}}{(\bar{U})} + \ldots\right] \qquad \text{III -16}$$

and combining equations III - 16 and III - 15,

$$\bar{P} = A + B\,\bar{U}^{\frac{1}{2}}\left[1 - \frac{1}{4}\frac{\overline{(u')^2}}{(\bar{U})} + \frac{1}{2}\frac{\overline{(v')^2}}{(\bar{U})} + \ldots\right] \qquad \text{III - 17}$$

Equation III - 17 shows the effect of velocity fluctuations on the mean power loss.

2. Heterogenous turbulent flow

The average power-velocity relationship for heterogenous turbulent flow is given by equation III - 14.

$$\bar{P} = \bar{A}(c) + \overline{B(c)V^{\frac{1}{2}}} \qquad \text{III - 14}$$

If the composition of the fluid past the hot wire is variable, the quantities A and B in the above equation will no longer be constant. The power input to the hot wire depends upon concentration as well as velocity past the sensor. The relationship between A and B and mean concentration is given below.

$$\bar{A} = \bar{A}(\bar{c} + c') = A(\bar{c}) + \frac{dA}{dc}\overline{c'} + \frac{d^2A}{dc^2}\frac{\overline{c'^2}}{2!} + \ldots$$

since the quantity $\overline{c'}$ is zero,

$$\bar{A} = A(\bar{c}) + \frac{d^2A}{dc^2}\frac{\overline{c'^2}}{2!} + \frac{d^3A}{dc^3}\frac{\overline{c'^3}}{3!} + \ldots \qquad \text{III-18}$$

The expression $BV^{\frac{1}{2}}$ can be expanded in a series. Thus,

$$BV^{\frac{1}{2}} = \left[B(\bar{c}) + \frac{dB}{dc}c' + \frac{d^2B}{dc^2}\frac{c'^2}{2!} + \ldots\right](\bar{U}^{\frac{1}{2}})\left(1 + \frac{1}{2}\frac{u'}{\bar{U}}\right.$$

$$\left. - \frac{1}{8}\frac{(u')^2}{(\bar{U})} + \frac{1}{4}\frac{(v')^2}{(\bar{U})} + \ldots\right) \qquad \text{III-19a}$$

After term by term multiplication and averaging, the above expression becomes:

$$\overline{BV^{\frac{1}{2}}} = B(\bar{c})\bar{U}^{\frac{1}{2}}\left[1 - \frac{1}{8}\frac{\overline{(u')^2}}{(\bar{U})} + \frac{1}{4}\frac{\overline{(v')^2}}{(\bar{U})} + \ldots\right]$$

$$+ \frac{dB}{dc}\bar{U}^{\frac{1}{2}}\left[\frac{1}{2}\frac{\overline{c'u'}}{\bar{U}} - \frac{1}{8}\frac{\overline{c'u'^2}}{\bar{U}^2} + \frac{1}{4}\frac{\overline{c'v'^2}}{\bar{U}^2} + \ldots\right]$$

$$+ \frac{d^2B}{dc^2}\bar{U}^{\frac{1}{2}}\left[\overline{c'^2} + \frac{1}{2}\frac{\overline{c'u'}}{\bar{U}} - \frac{1}{8}\frac{\overline{c'u'^2}}{\bar{U}^2} + \ldots\right]$$

The mean power velocity relationship is found by substituting equation III-18 and III-20 into equation III-17.

$$\bar{P} = A(\bar{c}) + \frac{d^2A}{dc^2}\frac{\overline{c'^2}}{2} + \ldots$$

$$+ B(\bar{c})\bar{U}^{\frac{1}{2}} \left[1 - \frac{1}{8}\frac{\overline{(u')^2}}{(\bar{U})} + \frac{1}{4}\frac{\overline{(v')^2}}{(\bar{U})} + \cdots\right]$$

$$+ \frac{dB}{dc}\bar{U}^{\frac{1}{2}} \left[\frac{1}{2}\frac{\overline{c'u'}}{\bar{U}} - \frac{1}{8}\frac{\overline{c'u'^2}}{\bar{U}^2} + \frac{1}{4}\frac{\overline{c'v'^2}}{\bar{U}^2} + \cdots\right]$$

$$+ \frac{d^2B}{dc^2}\bar{U}^{\frac{1}{2}} \left[\frac{\overline{c'^2}}{} + \frac{1}{2}\frac{\overline{c'u'}}{\bar{U}} - \frac{1}{8}\frac{\overline{c'u'^2}}{\bar{U}^2} + \cdots\right] \qquad \text{III-20}$$

Equation III-20 shows that the mean power loss may be greatly affected by density and velocity fluctuations. The velocity correction given by this equation may be very important in highly turbulent flows. It should also be noted that it reduces to equation III-17 if the concentration fluctuation is absent.

D. Relationships for Velocity and Density Fluctuations.

The real utility of hot wire anemometers is in the measurement of turbulent properties such as turbulence intensity and turbulent shear stress. As in velocity measurement, separate expressions for homogenous and heterogenous flow are obtained.

1. Homogenous flow.

In the preceding discussion, the following expression was obtained:

$$V^n = \bar{U}^n \left[1 + \frac{nu'}{\bar{U}} + \frac{n(n-1)(u')^2}{2(\bar{U})} + \frac{n(v')^2}{2(\bar{U})} + \cdots\right] \qquad \text{III-12}$$

This expression may then be substituted into equation III-1 to give the instantaneous power supplied to the sensor

$$\bar{P} + p' = A + B\bar{U}^{\frac{1}{2}} \left[1 + \frac{1}{2}\frac{u'}{\bar{U}} - \frac{1}{4}\frac{u'^2}{\bar{U}^2} + \frac{1}{2}\frac{v'^2}{\bar{U}^2} + \ldots\right] \quad \text{III-21}$$

The average power level $\bar{P}$ is given by equation III-17. Subtracting equation III-17 from equation III-21,

$$p' = B\bar{U}^{\frac{1}{2}} \left[\frac{1}{2}\frac{u'}{\bar{U}} + \frac{1}{4\bar{U}^2}\left(\overline{u'^2} - u'^2 + v'^2 - \overline{v'^2} + \ldots\right)\right] \quad \text{III-22}$$

Since the average values of p' and u' are zero, the root mean square (rms) values are normally used as a measure of turbulence. Defining $(\overline{u'^2})^{\frac{1}{2}}$ as the root mean square value of u' and $(\overline{p'^2})^{\frac{1}{2}}$ as the root mean square value of p', equation III-22 becomes

$$\overline{p'^2} = B^2\bar{U}\left[\frac{1}{4}\frac{(\overline{u'})^2}{(\bar{U})} + \frac{1}{4\bar{U}^3}\left(\overline{u'^3} + \overline{u'v'^2} + \ldots\right)\right] \quad \text{III-23}$$

Assuming that

$$u' << \bar{U}$$

$$v' << \bar{U}$$

equation III-23 may be linearized to give

$$\overline{p'^2} = \frac{B^2\bar{U}}{4}\frac{\overline{u'^2}}{\bar{U}^2}$$

or

$$\frac{2(\overline{p'^2})^{\frac{1}{2}}}{B\bar{U}^{\frac{1}{2}}} = \frac{(\overline{u'^2})^{\frac{1}{2}}}{\bar{U}} \qquad \text{III-24}$$

The quantity on the right hand side of this equation is known as the turbulence intensity. Thus, the turbulence intensity in the mean flow direction may be easily calculated from this relationship.

2. Heterogenous flow.

The power loss of the sensor is affected by changes in both velocity and concentration. In streams where the fluid medium is not homogeneous, the power loss fluctuations are a function of the density and velocity fluctuations and their cross product. Let us denote $\bar{P}$, $\bar{c}$, $\bar{U}$ as the mean power loss, density and velocity, respectively, and p', c', u' and v' as the fluctuations in power, density, and axial and transverse velocities. Then the instantaneous power loss is given by

$$P = \bar{P} + p' = A\,(\bar{c} + c') + B\,(\bar{c} + c')\left[\bar{U} + u')^2 + v'^2\right]^{\frac{1}{2}}$$

By expansion in a Taylor series,

$$\bar{P} + p' = A\,(\bar{c}) + \frac{dA}{dc}\,c' + \frac{1}{2!}\,\frac{d^2A}{dc^2}\,c'^2 + \ldots$$

$$+ \left[B\,(c) + \frac{dB}{dc}\,c' + \ldots\right]\left[\bar{U}^{\frac{1}{2}}\right]$$

$$\left[1 + \frac{1}{2}\frac{u'}{\bar{U}} - \frac{1}{8}\frac{u'^2}{\bar{U}^2} + \frac{1}{4}\frac{v'^2}{\bar{U}^2} + \ldots \right] \qquad \text{III-25}$$

Subtracting equation III-20 from equation III-25 gives

$$p' = \frac{dA}{dc}c' + \frac{dB}{dc}\bar{U}^{\frac{1}{2}}c' + \frac{B}{2}\frac{u'}{\bar{U}^{\frac{1}{2}}} + \frac{1}{2}\left[\frac{d^2A}{dc^2} + \frac{\bar{U}^{\frac{1}{2}}d^2B}{dc^2}\right]$$
$$\left[\overline{c'^2} - c'^2\right] - \frac{B}{8\bar{U}^{3/2}}\left[u'^2 - \overline{u'^2}\right] + \frac{B}{4\bar{U}^{3/2}}$$
$$\left[v'^2 - \overline{v'^2}\right] + \frac{1}{2}\frac{dB}{dc}\frac{1}{\bar{U}^{1/2}}\left[c'u' - \overline{c'u'}\right]$$
$$- \frac{1}{8}\frac{dB}{dc}\frac{1}{\bar{U}^{3/2}}\left[c'u'^2 - \overline{c'u'^2}\right] + \ldots \qquad \text{III-26}$$

Assuming that terms of order greater than one are negligible, equation III-26 reduces to

$$p' \approx \frac{dA}{dc}c' + \bar{U}^{1/2}\frac{dB}{dc}c' + \frac{B}{2\bar{U}^{1/2}}u' \qquad \text{III-27}$$

Equation III-27 is merely an approximation of equation III-26. It is valid only when the fluctuating quantities c' and u' are small. The above relation when used for flows where the turbulent intensity usually exceeds 10% will give an appreciable error.

Equation III-27 can also be derived using the tools of total derivatives. The exact differential dP is related to concentration and velocity by

$$dP = \frac{\partial P}{\partial c}dc + \frac{\partial P}{\partial V}dV$$

For small changes in c and V, $U \approx V$, $dP \approx p'$, $dc \approx c'$, and $du \approx u'$ so that,

$$p' = \frac{\partial P}{\partial c} c' + \frac{\partial P}{\partial V} u' \qquad \text{III-28}$$

Where $\frac{\partial P}{\partial c}$ and $\frac{\partial P}{\partial c}$ are obtained from King's equation (III-1)

$$p' = \left(\frac{dA}{dc} + \bar{U}^{\frac{1}{2}} \frac{dB}{dc}\right) c' + \frac{B}{2\bar{U}^{\frac{1}{2}}} u' \qquad \text{III-28a}$$

which is the same as equation III-26.

The average value of p' is zero and, normally, the root mean square (RMS) is used as a measure of the intensity of fluctuations. $(\overline{p'^2})^{\frac{1}{2}}$, $(\overline{c'^2})^{\frac{1}{2}}$, $(\overline{u'^2})^{\frac{1}{2}}$ are the root mean squares of power fluctuations, concentration fluctuations and velocity fluctuations, respectively.

Squaring equation III-27 and averaging with time, the following expression is obtained:

$$\overline{p'^2} = \frac{\partial P}{\partial c} \overline{c'^2} + 2 \frac{\partial P}{\partial c} \frac{\partial P}{\partial V} \overline{c' u'} + \left(\frac{\partial P}{\partial V}\right)^2 \overline{u'^2} \qquad \text{III-29}$$

Equation III-29 shows the relationship between the square of RMS of power, concentration, velocity fluctuations and the cross product $\overline{c'u'}$. Only the root mean square of the power fluctuations can be measured directly so that another two correlations are needed to evaluate the three terms.

These equations may be provided by applying equation III-29 to another sensor of different geometrical or physical characteristics as the first one and by applying equation III-29 to the sum and difference of the power loss in the two wires.

Thus, four different sets of equations may be obtained from the use of two hot-film sensors. Affixing the subscript $_1$ for the first film and $_2$ for the other film, the equation can be written as,

for the first sensor,

$$\overline{p_1'^2} = \left(\frac{\partial P_1}{\partial c}\right)^2 \overline{c'^2} + 2 \frac{\partial P_1}{\partial c} \frac{\partial P_1}{\partial V} \overline{c'u'} + \left(\frac{\partial P_1}{\partial V}\right)^2 \overline{u'^2} \qquad \text{III-30}$$

for the second sensor,

$$\overline{p_1'^2} = \left(\frac{\partial P_2}{\partial c}\right)^2 \overline{c'^2} + 2 \frac{\partial P_2}{\partial c} \frac{\partial P_2}{\partial V} \overline{c'u'} + \left(\frac{\partial P_2}{\partial V}\right)^2 \overline{u'^2} \qquad \text{III-31}$$

for the sum of power loss in the two wires

$$\overline{(p_1' + p_2')^2} = \left(\frac{\partial P_1}{\partial c} + \frac{\partial P_2}{\partial c}\right)^2 \overline{c'^2} + 2\left(\frac{\partial P_1}{\partial c} + \frac{\partial P_2}{\partial c}\right) \left(\frac{\partial P_1}{\partial V} + \frac{\partial P_2}{\partial V}\right) \overline{c'u'} + \left(\frac{\partial P_1}{\partial V} + \frac{\partial P_2}{\partial V}\right)^2 \overline{u'^2} \qquad \text{III-32}$$

for the difference of the two powers

$$\overline{(p_1' - p_2')^2} = \left(\frac{\partial P_1}{\partial c} - \frac{\partial P_2}{\partial c}\right)^2 \overline{c'^2} + 2\left(\frac{\partial P_1}{\partial c} - \frac{\partial P_2}{\partial c}\right)$$

$$\left(\frac{\partial P_1}{\partial V} - \frac{\partial P_2}{\partial V}\right) \overline{c'u'} + \left(\frac{\partial P_1}{\partial V} - \frac{\partial P_2}{\partial V}\right)^2 \overline{u'^2} \qquad \text{III-33}$$

Any three of the above four equations are in theory independent and may be used for calculating the three quantities $\overline{c'^2}$, $\overline{c'u'}$, and $\overline{u'^2}$. However, when the first two equations (III-30,-31) and either one of equations III-32 and -33 were applied in solving for the three unknowns, it was found that a slight change in any of the measured values $\overline{p_1'^2}$, $\overline{p_2'^2}$, $\overline{(p_1' + p_2')^2}$, or $\overline{(p_1' - p_2')^2}$ resulted in large changes in $\overline{c'^2}$ and $\overline{u'^2}$. It was also found that this occurred for changes in the measured values small enough to be beyond the sensitivity of the measuring apparatus.

The first observation comes from the fact that at high velocities,

$$\frac{\partial P_1}{\partial c} \Big/ \frac{\partial P_2}{\partial c} \approx \frac{\partial P_1}{\partial V} \Big/ \frac{\partial P_2}{\partial V}$$

(to be shown in a later section), i.e., if the three equations are written in the form,

$$a_1 \overline{c'^2} + b_1 \overline{c'u'} + c_1 \overline{u'^2} = P_1$$

$$a_2 \overline{c'^2} + b_2 \overline{c'u'} + c_2 \overline{u'^2} = P_2$$

$$a_3 \overline{c'^2} + b_3 \overline{c'u'} + c_3 \overline{u'^2} = P_3$$

then it will be found that

$$\frac{a_1}{a_2} \approx \frac{b_1}{b_2} \approx \frac{c_1}{c_2} \qquad \text{III-34}$$

$$\frac{a_1}{a_3} \approx \frac{b_1}{b_3} \approx \frac{c_1}{c_3} \qquad \text{III-35}$$

so that the determinant

$$\begin{vmatrix} a_1 & b_1 & c_1 \\ a_2 & b_2 & c_2 \\ a_3 & b_3 & c_3 \end{vmatrix}$$

is a very small quantity. Hence, slight changes in either of P_1, P_2, and P_3 produce large effects in the calculated values.

In view of the inability to obtain a valid solution from any three of the four equations, a different expression for the evaluation of $\overline{c'^2}$ is obtained from the power loss concentration relationship of the aspirator probe. Subtracting equation III-11 from equation III-10 results in

$$p' = \frac{dP}{dc} c' + \frac{d^2P}{dc^2} (c'^2 - \overline{c'^2}) + \frac{d^3P}{dc^3} (c'^3 - \overline{c'^3}) + \ldots \qquad \text{III-36}$$

squaring and time averaging the above equation,

$$\overline{p'^2} = \left(\frac{dP}{dc}\right)^2 \overline{c'^2} + 2\,\frac{dp}{dc}\,\frac{d^2P}{dc^2}\,\overline{c'^3} + 2\,\frac{dP}{dc}\,\frac{d^3P}{dc^3}\,\overline{c'^4} + \ldots \qquad \text{III-37}$$

and if it can be assumed that the higher order terms are negligible, equation III-37 reduces to

$$\overline{c'^2} = \frac{\overline{p'^2}}{\left(\frac{dP}{dc}\right)^2} \qquad \text{III-38}$$

Equation III-38, together with equation III-30 and III-31, may be used for obtaining $\overline{c'^2}$, $\overline{u'^2}$, and $\overline{c'u'}$. It was found, however, that these equations give results which exhibited a lack of dependence of $\overline{u'^2}$ and $\overline{c'^2}$, i.e., $\overline{u'^2}$ is not greatly affected by whatever values are found in equation III-38. This observation will be shown to be mathematically correct.

Equation III-30 and III-31 may be written in the form

$$a_1\,\overline{c'^2} + b_1\,\overline{c'u'} + c_1\,\overline{u'^2} = P_1 \qquad \text{III-39}$$

$$a_2\,\overline{c'^2} + b_1\,\overline{c'u'} + c_2\,\overline{u'^2} = P_2 \qquad \text{III-40}$$

By a rearrangement and division equations III-39 and III-40 become

$$\frac{a_1 \overline{c'^2} + b_1 \overline{c'u'}}{a_2 \overline{c'^2} + b_2 \overline{c'u'}} = \frac{P_1 - c_1 \overline{u'^2}}{P_2 - c_2 \overline{u'^2}} \qquad \text{III-41}$$

In order for the turbulent velocity term $\overline{u'^2}$ to be independent of $\overline{c'^2}$, the left hand side of the equation should have a constant value, whatever may be the value of $\overline{c'^2}$. This can be shown to be true if

$$\frac{a_1}{a_2} = \frac{b_1}{b_2}$$

That this equality is almost satisfied at region of high velocity will be shown in the following paragraph.

From previous discussion, the following may be obtained.

$$a_1 = \left(\frac{dA_1}{dc} + \frac{dB_1}{dc} V^{\frac{1}{2}}\right)^2 \qquad \text{III-42}$$

$$a_2 = \left(\frac{dA_2}{dc} + \frac{dB_2}{dc} V^{\frac{1}{2}}\right)^2$$

$$= \left(k_1 \frac{dA_1}{dc} + k_2 \frac{dB_1}{dc} V^{\frac{1}{2}}\right)^2 \qquad \text{III-43}$$

$$b_1 = \left(\frac{dA_1}{dc} + \frac{dB_1}{dc}\right) \frac{B_1}{V^{\frac{1}{2}}} \qquad \text{III-44}$$

$$b_2 = \left(\frac{dA_2}{dc} + \frac{dB_2}{dc}\right) \frac{B_2}{V^{\frac{1}{2}}}$$

$$= \left(k_1 \frac{dA_1}{dc} + k_2 \frac{dB_1}{dc}\right) \frac{k_2 B_1}{V^{\frac{1}{2}}} \qquad \text{III-45}$$

From equations III-43 and III-42,

$$\frac{a_1}{a_2} = \frac{1}{k_2^2}\left[\frac{\frac{dA_1}{dc} + \frac{dB_1}{dc} V^{\frac{1}{2}}}{\frac{k_1}{k_2}\frac{dA_1}{dc} + \frac{dB_1}{dc} V^{\frac{1}{2}}}\right]^2 \qquad \text{III-46}$$

Dividing equation III-44 by equation III-45

$$\frac{b_1}{b_2} = \frac{1}{k_2^2}\left[\frac{\frac{dA_1}{dc} + \frac{dB_1}{dc} V^{\frac{1}{2}}}{\frac{k_1}{k_2}\frac{dA_1}{dc} + \frac{dB_1}{dc} V^{\frac{1}{2}}}\right] \qquad \text{III-47}$$

$$\frac{c_1}{c_2} = \frac{1}{k_2^2} \qquad \text{III-48}$$

At moderately high velocities, where

$$\frac{dB_1}{dc} V^{\frac{1}{2}} >> \frac{k_1}{k_2}\frac{dA_1}{dc}, \quad \frac{a_1}{a_2} \approx \frac{b_1}{b_2}$$

which proves that $\overline{c'^2}$ is almost independent of $\overline{u'^2}$.

Though it can be said that since the following equation also holds

$$\frac{a_1 \overline{c'^2} + c_1\overline{u'^2}}{a_1 \overline{c'^2} + c_2\overline{u'^2}} \qquad \frac{P_1 - b_1 \overline{c'u'}}{P_2 - b_2 \overline{c'u'}} \qquad \text{III-49}$$

and that at high velocities $\frac{a_1}{a_2} \approx \frac{c_1}{c_2}$, then $\overline{c'u'}$

should also be constant. This is true. However, the term $\overline{c'u'}$ will not be as close to its original value as $\overline{u'^2}$ since the ratio $\frac{a_1}{a_2}$ is closer to $\frac{b_1}{b_2}$ than it is to $\frac{c_1}{c_2}$.

As a final word, equations III-42, III-43, and III-45 also show that equations III-39 and III-40 are not independent of each other at very high velocities, because at this point

$$a_1 \overline{c'^2} + b_1 \overline{c'u'} + c_1 \overline{u'^2} = P_1 =$$

$$\frac{1}{k_2^2} \left[a_2 \overline{c'^2} + b_2 \overline{c'u'} + c_2 \overline{u'^2} \right]$$

It will be discussed in Chapter VI that the fluctuations in density, as given by equation III-38, do not represent the true fluctuations in the flow field because of a damping effect in the aspirator probe. The results of applying equations III-38, III-31 and III-30 in the calculations forms the basis of discussion in Chapter VI and will not be further discussed in this section.

IV EXPERIMENTAL DISCUSSION

Figure IV.1 shows the experimental setup used in obtaining data. Essentially, it consists of a 4 foot long, 3/4 inch diameter stainless steel tube mounted coaxially in a 6 foot vertical plexiglass duct of square cross section. A centrifugal blower with its inlet connected to the bottom of the duct pulls the outer stream air through the duct and metered, constant temperature Freon-12 is pressure fed through the 3/4 inch steel tube as the inner jet. Hot wire anemometers are mounted on a traversing mechanism geared to the duct to traverse the field radially and axially, and their power outputs are controlled by two independent channels and recorded on a digital voltmeter. The monitoring equipment included a digital voltmeter, rms voltmeter, a sum and difference unit that could add or subtract the outputs from the two independent channels and a dual beam oscilloscope.

Most of the sensors used in the experiment are of the hot film type. For the experiment, two sensor probes were used. They were a parallel wire probe and an aspirator probe. In the parallel wire probe, two sensors, .01 inch apart, are mounted parallel to each other on a single probe. The wires were oriented in a plane perpendicular to the plane of the traversing mechanism and were connected to the probe holder by a ninety degree angle adapter. The aspirator probe is a concentration measuring device and consists of a 1 mil sensor mounted inside a 0.08 inch ID tube. The tube is connected to

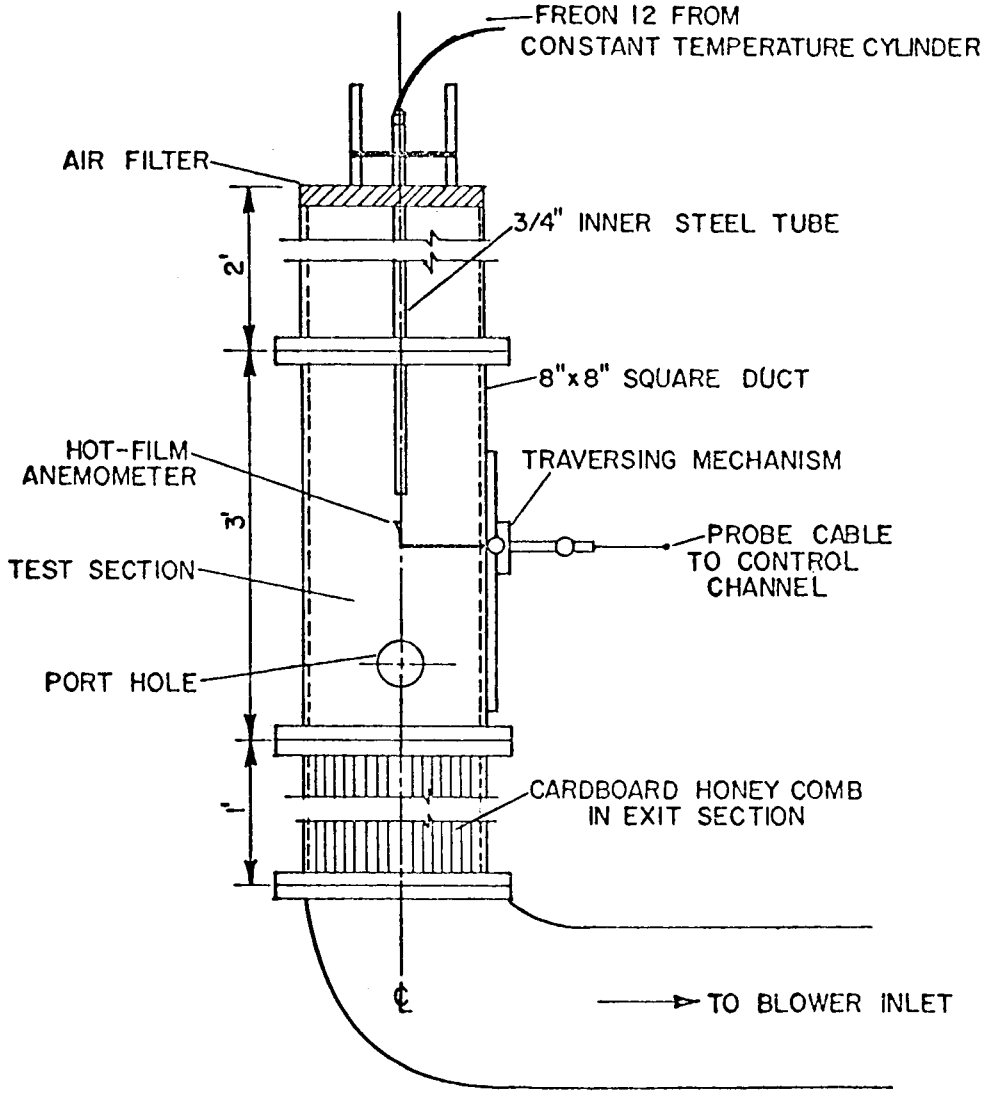

FIG. IV .1 TEST SECTION

an angle adapter and then to the probe holder. The tube contains a jewel bearing with a hole diameter of 0.008 $\pm$ .001 inch behind the film. A vacuum pump sucks through the probe holder and sufficiently reduces the pressure downstream from the bearing to insure sonic velocity at the throat of the bearing. This sonic velocity depends on the molecular weight of the gas and, therefore, on the composition. The power dissipated at the film depends on the composition and velocity of the gas passing through. The velocity past the film is related to the sonic velocity by the equation of continuity, and since this depends on concentration, the power dissipated from the film is related directly to concentration. The device withdraws only a small sample from the stream and provides instantaneous readings at the point of interest.

Before making any measurements, the sensors are calibrated by passing a stream of gas of known velocity and concentration through them. Power loss readings at different velocities and concentrations are taken. A graph of millivolts registered versus gas velocity and density is drawn and is shown in Figures IV-2 and IV-3, respectively. (See Zawacki[3]).

Experimental procedure:

A set of data for a particular inner stream to outer stream velocity ratio included four runs: (1) a run with the aspirator probe to determine density profiles; (2) a second run with the signal from the aspirator probe connected to the rms voltmeter to give fluctuating density measurements;

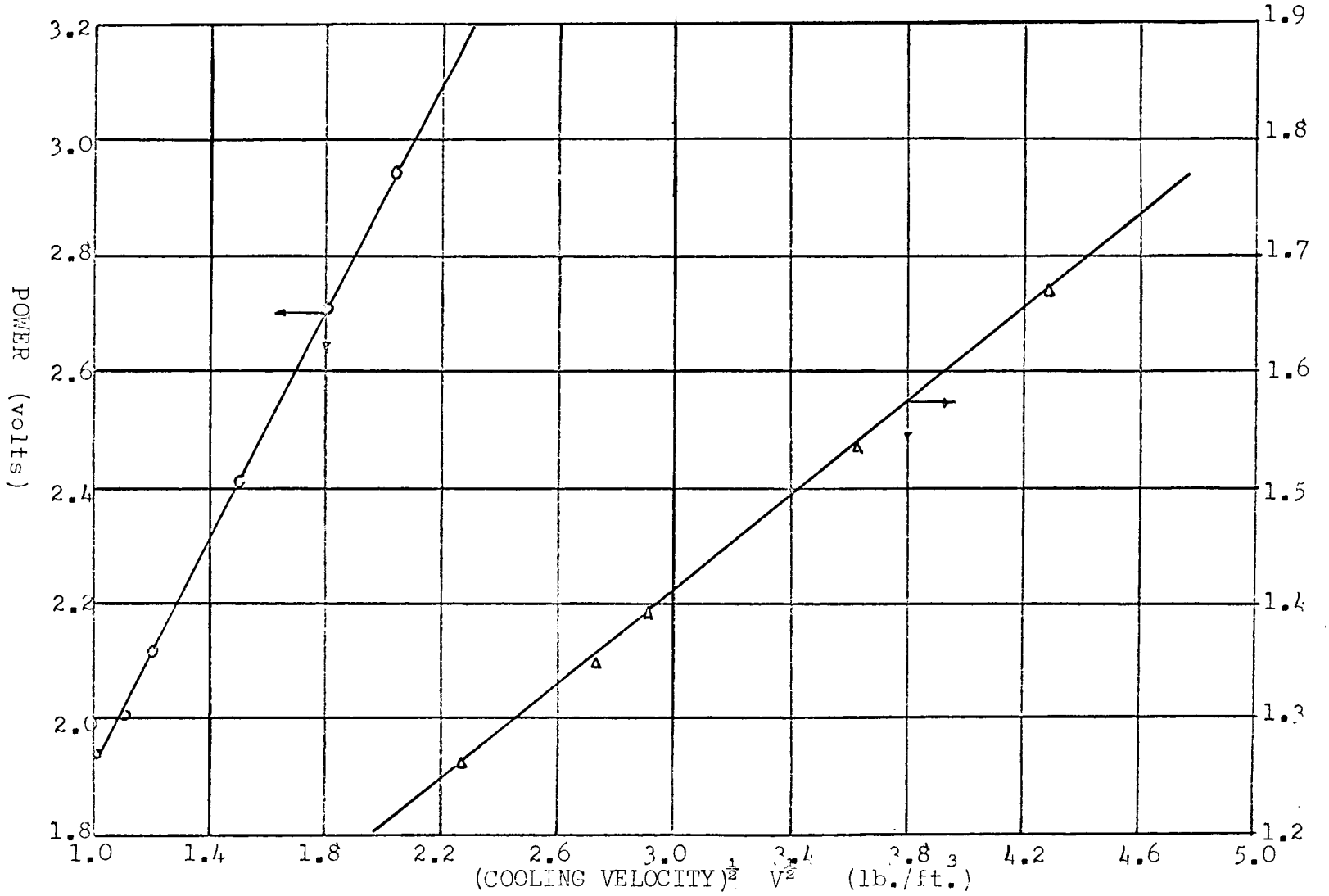

FIGURE IV-2 VELOCITY CALIBRATION CURVE

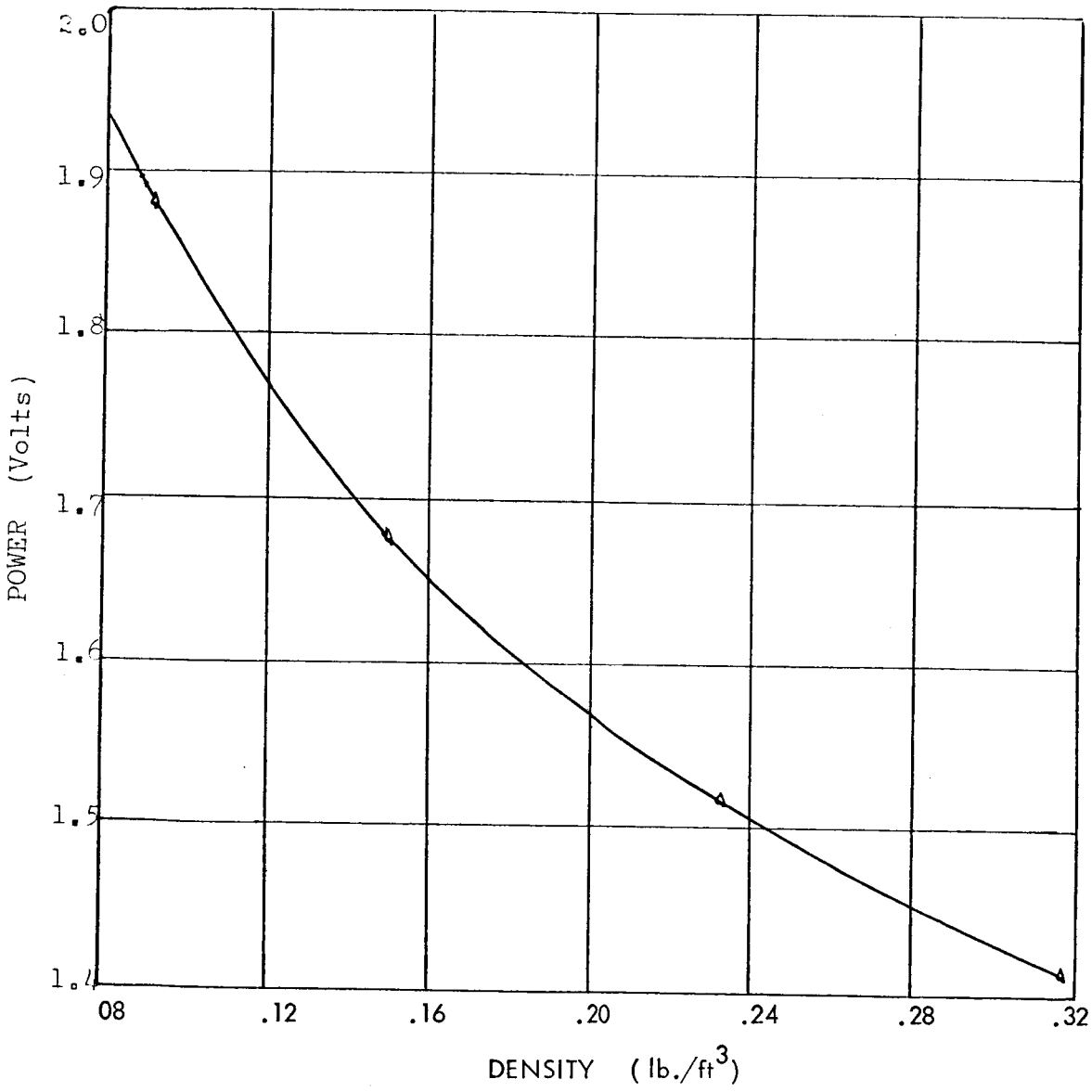

FIGURE IV-3 POWER DENSITY CALIBRATION CURVE

(Density Calibration curve)

(3) the third run is made with a parallel wire probe to determine average velocity profiles; (4) for the fourth run, the outputs from the sensors of the parallel wire are transmitted to the rms voltmeter and the fluctuating voltage recorded.

A more detailed treatment of the experimental work is given by D'Souza[25].

V CALCULATION PROCEDURE

From the data collected, the velocity $\bar{U}$, density $\bar{\rho}$, and fluctuating quantities $\overline{\rho'^2}$, $\overline{\rho'u'}$, and $\overline{u'^2}$ are determined. The density ρ is used because it is more convenient to express concentration in terms of density.

The following calibration curves are required for processing the experimental data:

a. Calibration curve for the aspirator probe, which gives the relation between power input and density, from here on will be called density calibration curve.

b. Power versus square root of velocity graphs for various freon air - gas mixtures, for both sensors on the parallel wire probe, from here on will be called velocity calibration curve.

c. Subsequent "A" - versus - density and "B" - versus - density curves as shown in Figure V-1, which are called the A - calibration curve and B - calibration curve, respectively.

The power input to the aspirator probe is directly converted to density from the density calibration curve. The power loss correction for fluctuating densities as given by equation III-11 was not applied. However, this correction was found to be small as will be mentioned in a later section. This correction equation is given below in terms of density ρ.

$$\bar{P}_d - \frac{d^2P}{d\rho^2}\overline{d\rho'^2} - \frac{d^3P}{d\rho^3}\overline{d\rho'^3} - \ldots = P_d(\bar{\rho}) \qquad \text{V-1}$$

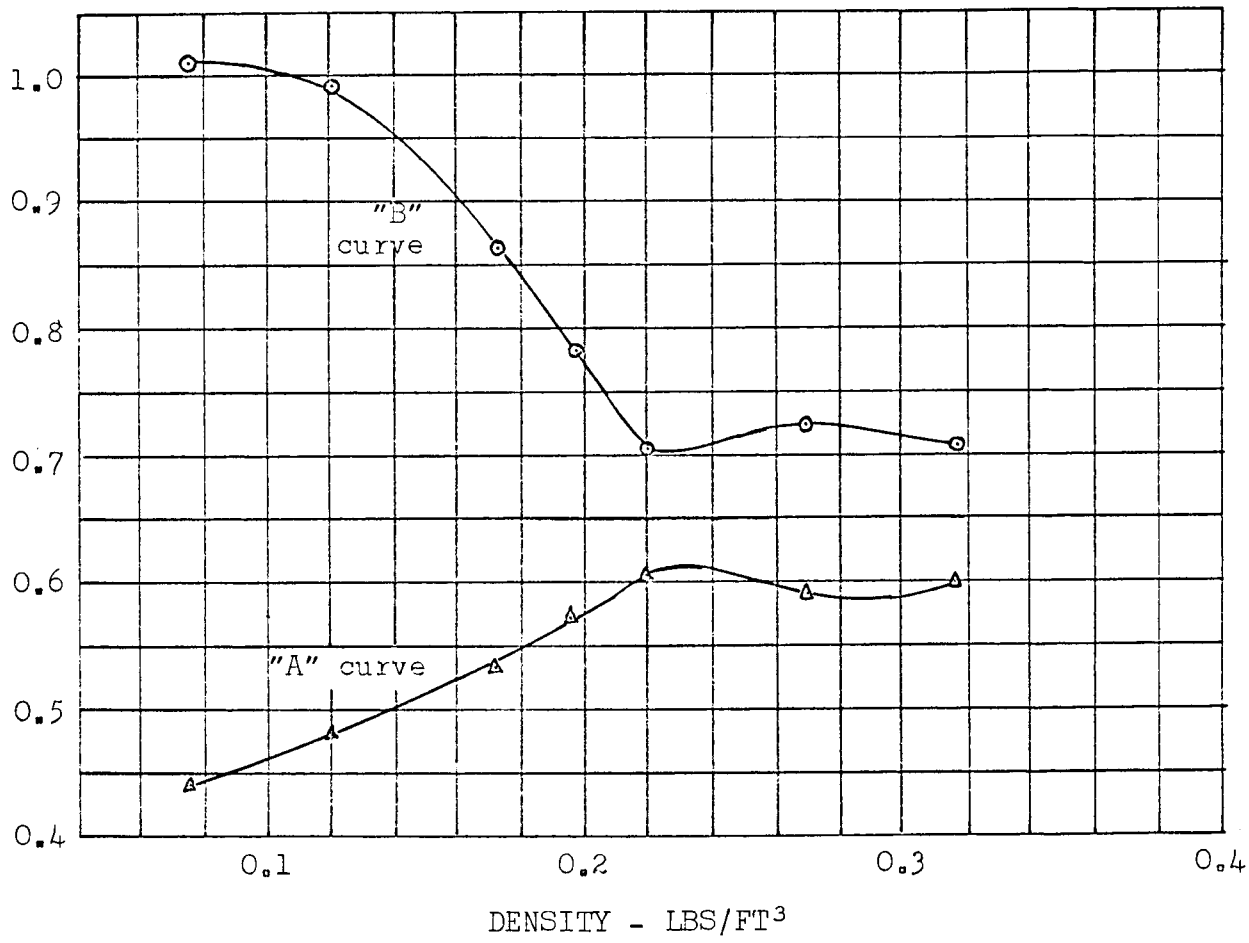

FIGURE V-1 SLOPE "B" AND INTERCEPT "A" AS A FUNCTION OF DENSITY

Where P_d refers to the measured mean power loss in run 1, $P_d(\bar{\rho})$ refers to the power loss corresponding to the actual mean density in the density calibration curve.

It is sufficient to use only the first term in the correction, because the other terms were found to be very small compared to the first one.

The square of the rms of density fluctuation $\overline{\rho'^2}$ is found from equation III-37 which, in view of the contents of the preceding paragraph, simplifies to

$$\overline{p_d'^2} = \left(\frac{dP_d}{d\rho}\right)^2 \overline{\rho'^2}$$

and by a rearrangement

$$\overline{\rho'^2} = \frac{\overline{p_d'^2}}{\left(\frac{dP_d}{d\rho}\right)^2} \qquad \text{V-2}$$

Where $\overline{\rho'^2}$ is the square of the rms of fluctuations in density obtained in run 2 and $\frac{dP_d}{d\rho}$ is the slope of the density calibration curve.

In order to determine the velocity at a point in the flow field, the density at that point is required. From the A and B calibration curves the values of A and B are read. With the average power supplied to the 2 mil sensor at that point and the simplified form of equation III-1 as given below, the velocity is calculated.

$$P = A + BV^{\frac{1}{2}} \qquad \text{V-3}$$

The correction for velocity given in equation III-20 is not used, and it should be expected that errors exist in the calculated values where fluctuations are quite large. The difference between calculated mean velocity and the actual mean axial velocity ($\bar{U}$) can be derived from equation III-20 and is given below:

$$U_{\text{calculated}} = \bar{U}\left[1 - \frac{1}{4}\frac{\overline{u'^2}}{\bar{U}^2} + \frac{1}{2}\frac{\overline{v'^2}}{\bar{U}^2} + \frac{1}{B}\frac{dB}{d\rho}\left(\frac{\overline{\rho'u'}}{\bar{U}} - \frac{1}{4}\frac{\overline{\rho'u'^2}}{\bar{U}^2} + \frac{1}{2}\frac{\overline{\rho'v'^2}}{\bar{U}^2}\right) + \frac{1}{B}\left(\frac{1}{\bar{U}^2}\frac{d^2A}{d\rho^2} + \frac{d^2B}{d\rho^2}\right)\overline{\rho'^2} + \ldots\right] \qquad \text{V-4}$$

Turbulent intensities as large as 20% can be shown to give an error of about 1%. For instance, in the above case, the terms

$$\frac{\overline{u'^2}}{\bar{U}^2} \quad \text{and} \quad \frac{\overline{v'^2}}{\bar{U}^2}$$

can be assumed to be both equal to 0.04. Since the rest of the turbulence terms containing density are negligible compared to the velocity fluctuations, then

$$U_{\text{calculated}} = \bar{U}\left[1 - \frac{.04}{4} + \frac{.04}{2}\right] = 1.01\,\bar{U} \qquad \text{V-5}$$

Equation V-4 shows that velocity corrections are negligible for turbulence intensities as high as 20%.

The other two fluctuating quantities, $\overline{\rho' u}$ and $\overline{u'^2}$, are found from equations III-30 and III-31. Rewriting them in terms of density:

$$\overline{p_1'^2} = \left(\frac{\partial P_1}{\partial \rho}\right)^2 \overline{\rho'^2} + 2 \frac{\partial P_1}{\partial \rho} \frac{\partial P_1}{\partial V} \overline{\rho' u'} + \left(\frac{\partial P_1}{\partial V}\right)^2 \overline{u'^2} \qquad \text{V-6}$$

$$\overline{p_1'^2} = \left(\frac{\partial P_2}{\partial \rho}\right)^2 \overline{\rho'^2} + 2 \frac{\partial P_2}{\partial \rho} \frac{\partial P_2}{\partial V} \overline{\rho' u'} + \left(\frac{\partial P_2}{\partial V}\right) \overline{u'^2} \qquad \text{V-7}$$

$\overline{p_1'^2}$ and $\overline{p_2'^2}$ are obtained when the rms signals from the two mil film and the 0.15 mil wire are squared.

To calculate

$$\frac{\partial P_1}{\partial \rho} \quad \text{and} \quad \frac{\partial P_2}{\partial \rho} ,$$

the quantities

$$\frac{dA}{d\rho} \quad \text{and} \quad \frac{dB}{d\rho}$$

are first evaluated. This is done by formulating a twenty degree polynomial for the A and B calibration curves, and

$$\frac{dA}{d\rho} \quad \text{and} \quad \frac{dB}{d\rho}$$

are calculated by taking the termwise derivative of the polynomial. Only the polynomial expression for one wire is needed since A_1 and B_1 are linearly related to A_2 and B_2, respectively.

Equations V-5 and V-6 are solved simultaneously, and then

$$\frac{(\overline{\rho'^2})^{\frac{1}{2}}}{\bar{\rho}} \quad , \quad \frac{(\overline{u'^2})^{\frac{1}{2}}}{\bar{U}} \quad , \text{ and } \quad \frac{\overline{\rho'u'}}{(\overline{\rho'^2})^{\frac{1}{2}}\,(\overline{u'^2})^{\frac{1}{2}}}$$

are subsequently obtained. A sample calculation is given in D'Souza's thesis[25] and is reprinted in the following pages.

A sample calculation for 4F run is shown below. Axial position 2.0". The concentration profile was first determined with an aspirator probe. The digital voltmeter readings are shown below.

radius 'r'	0"	0.05"	0.1"	0.2"	0.3"	0.4"	0.5"	1.0"
volt read:	1.415	1.422	1.446	1.604	1.764	1.875	1.962	1.962

From a graph of Figure IV.3 these readings were converted to densities.

radius 'r'	0"	0.05"	0.1"	0.2"	0.3"	0.4"	0.5"	1.0"
density ρ lb/ft^3	0.317	0.3095	0.287	0.183	0.121	0.191	0.075	0.075

Figure IV.3 was approximated by a polynomial of the form $1.962 - 1.153\,x + 1.017\,x^2 - 0.396\,x^3$ $\left(x = \frac{d - .075}{.225}\right)$

The quantity $\left[\frac{\partial f(\rho)}{\partial \rho}\right]$ at any density was determined by taking the derivative of the polynomial at that density.

The fluctuating voltage registered by the aspirator probe was used in equation V-2 to give $\overline{\rho'^2}$

radius r"	0"	0.05"	0.1"	0.2"	0.3"	0.4"	0.5"	1.0"
(r.m.s. voltage) asp	0.0086	0.0160	0.0384	0.064	0.0601	0.0475	0.00225	0.0032
$\frac{\overline{\rho'^2}}{\bar{\rho}}$	0.0209	0.0414	0.1133	0.2303	0.1699	0.1225	0	0

The values of 'A' and 'B' in equation V-3 are determined from graphs as in Figure V.1. With these values and the average voltage recorded by the 2 mil sensor the velocity profile was calculated.

radius:	0"	0.05"	0.01"	0.02"	0.03"	0.04"	0.05"	1.0"
Avg. volt. read.	2.530	2.525	2.518	2.674	3.140	3.600	3.870	4'084
'A'	0.6625	0.669	0.685	0.8275	0.962	0.990	1.0	1.0
'B'	1.56	0.5568	0.557	0.511	0.4505	0.427	0.415	0.415
Velocity	11.12	11.11	11.07	13.06	23.37	37.36	47.82	55.22

The fluctuating voltages used in equations V-6 and V-7 were:

radius	0"	0.05"	0.1"	0.2"	0.3"	0.4"	0.5"	1.0"
$\overline{p'^2_1}$	.002718	.002954	.004684	.02185	.04156	.0334	.01465	.00188
$\overline{p'^2_2}$	.0002859	.0003312	.0005860	.00425	.006741	.00570	.002498	.000232

The following turbulence intensities were obtained:

radius	0"	.05"	0.1"	0.2"	0.3"	0.4"	0.5"	1.0"
$\frac{\overline{u'^2}}{\overline{U}}$	0.0476	0.0508	0.0584	0.2146	0.3401	0.3447	0.0841	0.0277

Computer Programming

A program for the calculations was written in Fortran IV language and was run in a 360 computer system. The inputs to the program consist of:

(1) Axial and radial positions at which data are taken.

(2) Manually computed values of density and velocity at these points.

(3) rms values of the power loss in the aspirator probe. (data from run 2)

(4) rms values of the power loss in each of the two sensors of the parallel wire probe. (data from run 4)

(5) Coefficients of the polynomial expansion of the A and B calibration curves. These coefficients were obtained from the output of a SINPAK subroutine program that is available in the built-in library of most computers.

(6) Four points from the density calibration curve taken at equal intervals. These points are to be used in a four term polynomial approximation of the density calibration curve, formulated as shown below.

$$P = D_0 + D_1 y + D_2 y^2 + D_3 y^3 \qquad \text{V-8}$$

If the four points are (P_1, ρ_1), (P_2, ρ_2), (P_3, ρ_3), and (P_4, ρ_4), respectively, then

$$y = \frac{\rho - \rho_1}{\rho_4 - \rho_1} \qquad \text{V-9}$$

$$C_0 = P_1$$

$$C_3 = (P_4 - 3 \times P_3 + 3 \times P_2 - P_1) \times \frac{3^3}{6}$$

$$C_2 = -C_3 \times 6 \times 3^3 + P_3 - 2 \times P_2 - P_1) \times \frac{3^3}{6} \quad \text{V-10a,b,c,d}$$

$$C_1 = P_4 - C_0 - C_2 - C_3$$

A flow chart of the program is shown below:

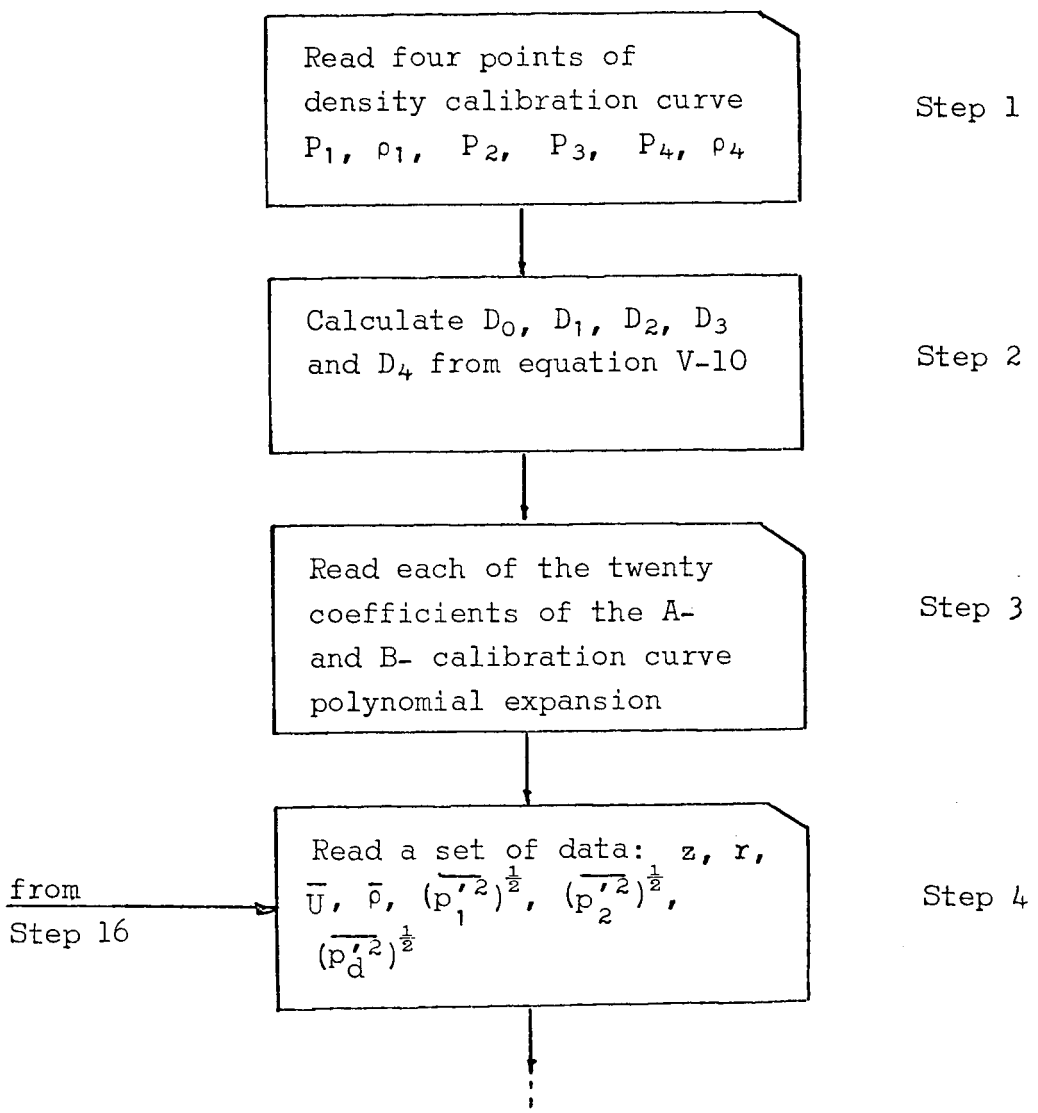

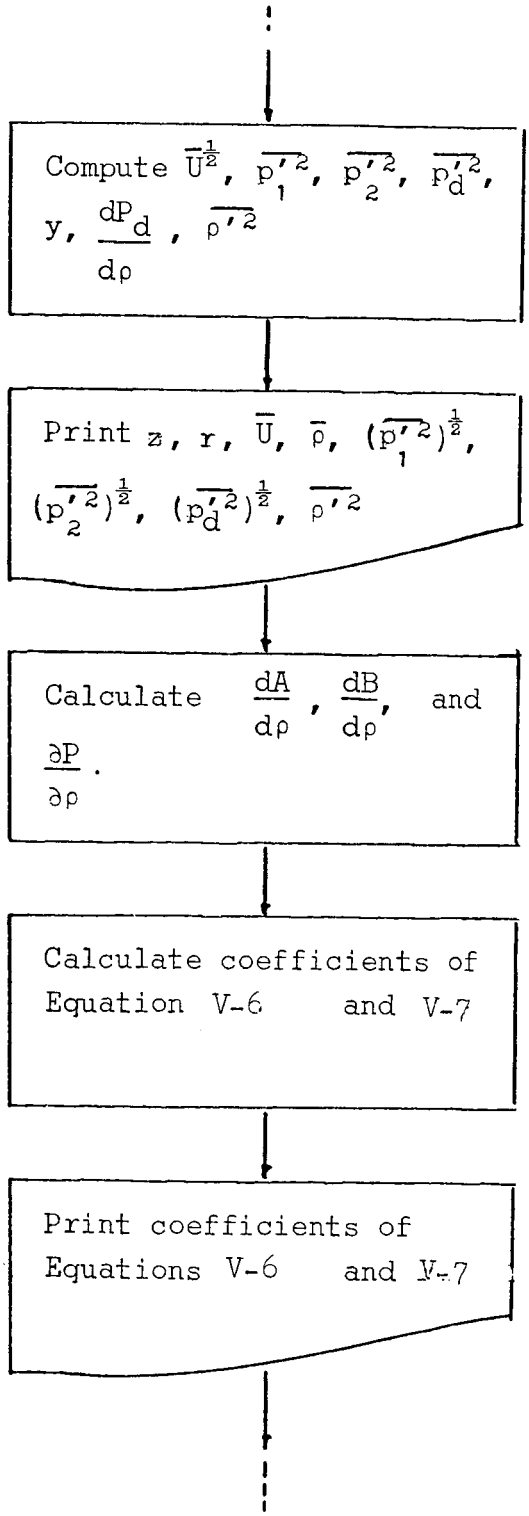
Compute $\overline{U}^{\frac{1}{2}}$, $\overline{p_1'^2}$, $\overline{p_2'^2}$, $\overline{p_d'^2}$, y, $\frac{dP_d}{d\rho}$, $\overline{\rho'^2}$
Step 5
Print z, r, $\overline{U}$, $\overline{\rho}$, $(\overline{p_1'^2})^{\frac{1}{2}}$, $(\overline{p_2'^2})^{\frac{1}{2}}$, $(\overline{p_d'^2})^{\frac{1}{2}}$, $\overline{\rho'^2}$
Step 6
Calculate $\frac{dA}{d\rho}$, $\frac{dB}{d\rho}$, and $\frac{\partial P}{\partial \rho}$.
Step 7
Calculate coefficients of Equation V-6 and V-7
Step 8
Print coefficients of Equations V-6 and V-7
Step 9

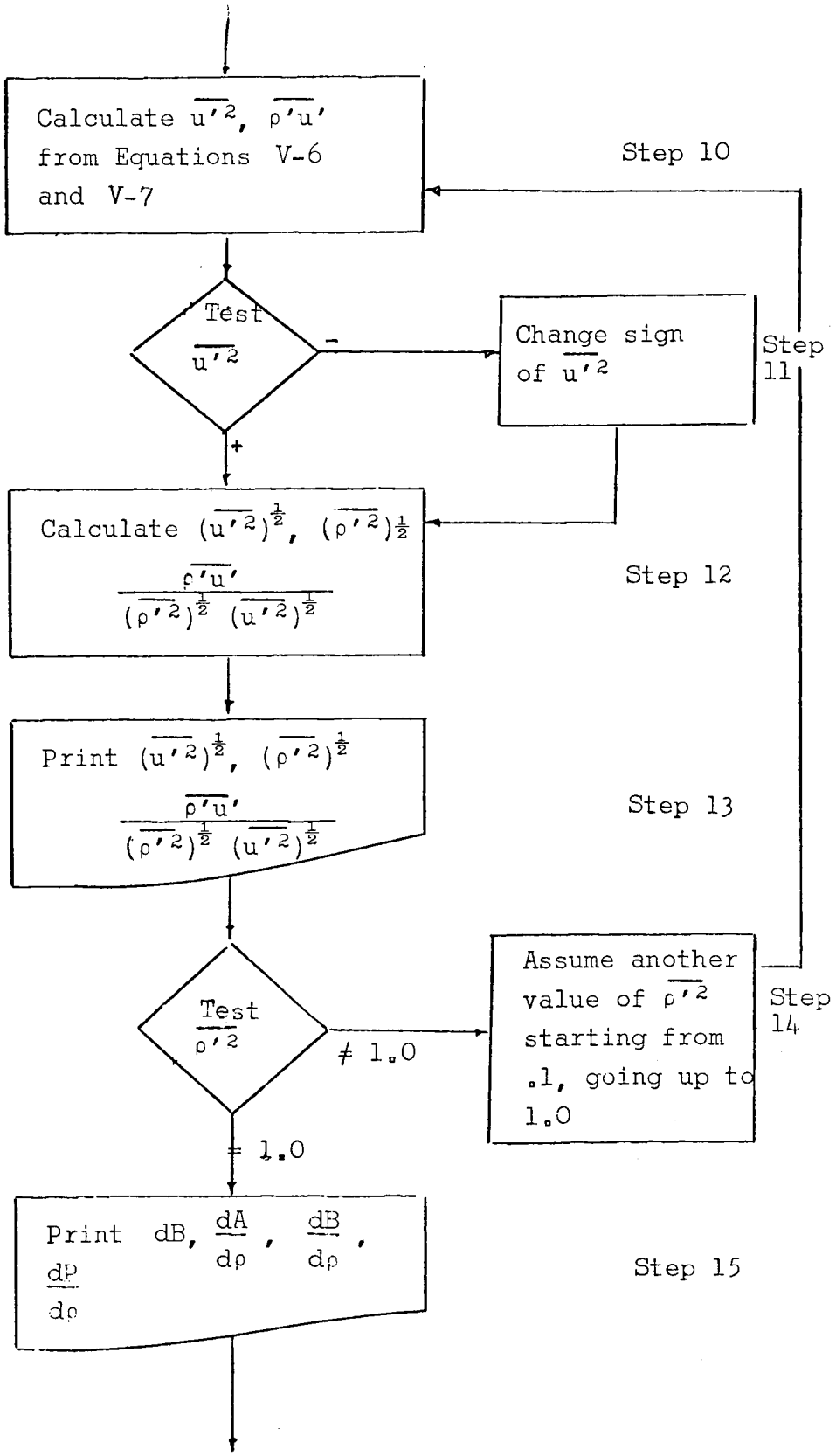
Calculate $\overline{u'^2}$, $\overline{\rho'u'}$ from Equations V-6 and V-7
Step 10
Test $\overline{u'^2}$
−
Change sign of $\overline{u'^2}$
Step 11
+
Calculate $(\overline{u'^2})^{\frac{1}{2}}$, $(\overline{\rho'^2})^{\frac{1}{2}}$, $\frac{\overline{\rho'u'}}{(\overline{\rho'^2})^{\frac{1}{2}}\,(\overline{u'^2})^{\frac{1}{2}}}$
Step 12
Print $(\overline{u'^2})^{\frac{1}{2}}$, $(\overline{\rho'^2})^{\frac{1}{2}}$, $\frac{\overline{\rho'u'}}{(\overline{\rho'^2})^{\frac{1}{2}}\,(\overline{u'^2})^{\frac{1}{2}}}$
Step 13
Test $\overline{\rho'^2}$
$\neq 1.0$
Assume another value of $\overline{\rho'^2}$ starting from .1, going up to 1.0
Step 14
$= 1.0$
Print dB, $\frac{dA}{d\rho}$, $\frac{dB}{d\rho}$, $\frac{dP}{d\rho}$
Step 15

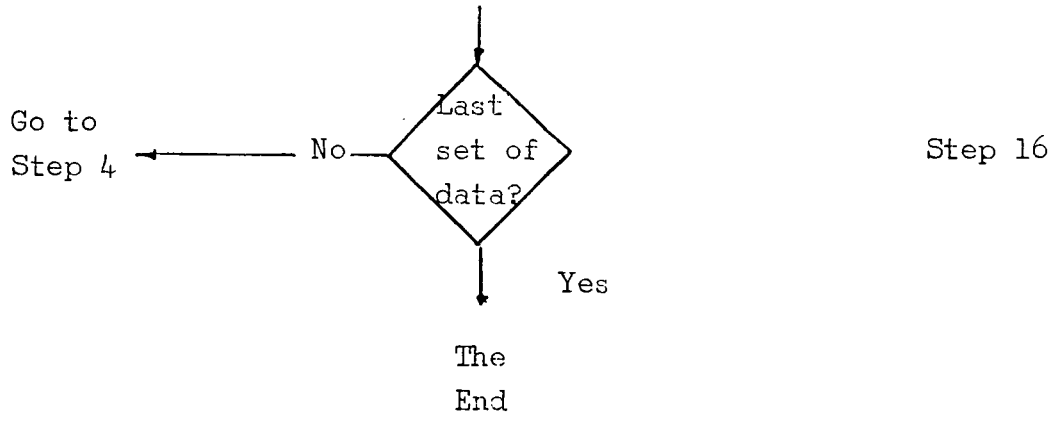

Explanation of computer flow chart

Step 1 - Stores values of the ordinates, P_1, P_2, P_3, P_4 of the four points taken from density calibration curve and the abscissa of the first and last point, ρ_1 and ρ_2, respectively. The abscissa of the second and third point need not be stored.

Step 2 - Self explanatory

Step 3 - Self explanatory

Step 4 - Each set of data consists of the axial position z, radial position r, velocity $\bar{U}$, density $\bar{\rho}$, rms of power loss in first wire $(\overline{p_1'^2})^{\frac{1}{2}}$, rms of power loss in second wire $(\overline{p'^2})^{\frac{1}{2}}$ and rms of power loss in aspirator probe $(\overline{p_d'^2})^{\frac{1}{2}}$. These data are taken from a single point in the flow field.

Step 5 - In this step, the computer takes the square root of $\bar{U}_1$, squares the three rms inputs, calculate

$\frac{dP_d}{d\rho}$ from equations V-8 and 9 and calculate $\overline{\rho'^2}$ from equation V-2 and the term y from equation V-9.

Step 6 - Self explanatory.

Step 7 - The derivative with respect to density of A and B is found by a termwise differentiation of its polynomial expression. The derivative of power with respect to density is subsequently obtained from the equation given below

$$\frac{\partial P}{\partial \rho} = \frac{dA}{d\rho} + \frac{dB}{d\rho} V^{\frac{1}{2}}$$

Step 8 - The coefficients of equations V-6 and V-7 are easily found from the previous calculations.

Step 9 - Self explanatory

Step 10 - $\overline{u'^2}$ and $\overline{\rho'u'}$ are calculated by direct substitution method.

Step 11 - The sign of $\overline{u'^2}$ is changed to positive because the computer will give an error message if the square root of a negative number is taken.

Step 12 - Self explanatory

Step 13 - Self explanatory

Step 14 - The values of $\overline{u'^2}$ and $\overline{\rho'u'}$ are calculated for diffrent values of $\overline{\rho'^2}$. The computer starts with the

value obtained from equation V-2 and then subsequently assumes values of 0.1, 0.2 and up to 1.0 for $\overline{\rho'^2}$. The reason for doing this is explained in Chapter VI.

Step 15 - Self explanatory

Step 16 - Self explanatory

VI RESULTS AND DISCUSSION

This chapter deals with the presentation of results which were obtained from the data and calculations as described in the previous chapters. An analysis of the values of velocity and density fluctuations obtained, as well as an explanation of observed peculiarities in the behavior of density and velocity profiles are included in the discussion.

A. Density and Velocity Fluctuations

From the results of the calculations, it was observed that

(1) In regions of low velocity, the correlations used for obtaining fluctuating terms give erratic results, such as a negative sign for $\overline{u'^2}$. A simple reason for this occurrence is that the correlations are not applicable at low velocities. This explanation is supported by the behavior of data points in the power-velocity calibration curves which shows that at low velocities, the power required ceases to be a function of density and becomes dependent on velocity only. (See Figure VI-1)

(2) In regions of high velocities, reasonable values of $\overline{\rho'^2}$ and $\overline{u'^2}$ are obtained, but the values for $\overline{\rho'u'}$ are found to be impossible. When the density fluctuation ($\overline{\rho'^2}$) is increased by steady amounts and then used in calculating $\overline{\rho'u'}$ and $\overline{\rho'^2}$, it was observed that an increase

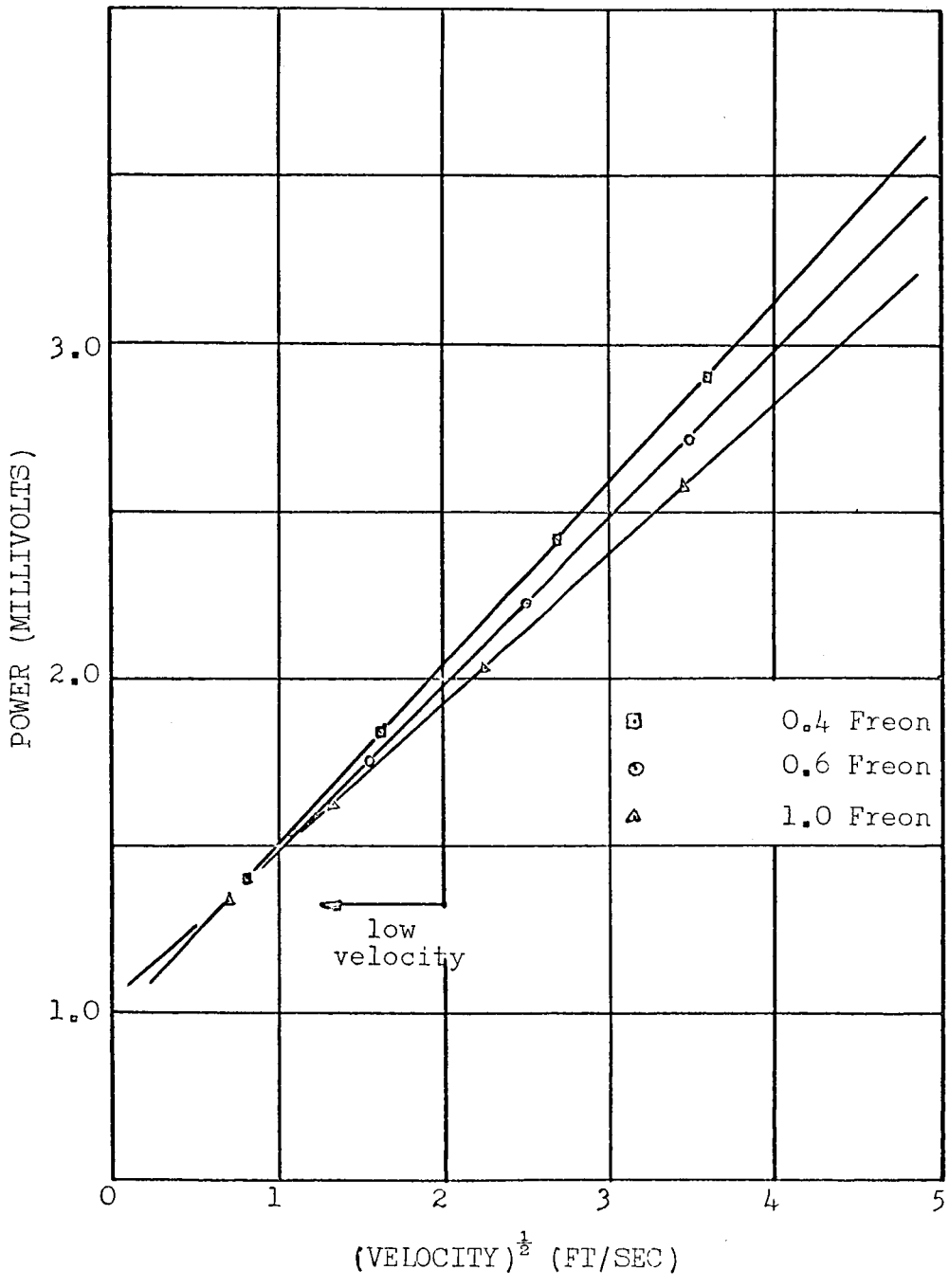

FIGURE VI-1 POWER VELOCITY RELATIONSHIP AT DIFFERENT AIR FREON MIXTURE

in the density fluctuation of 150% barely changed the turbulence intensity by 8%. It was also observed that while the cross product $\overline{\rho' u'}$ would have a ridiculous value initially, subsequent values obtained by increasing $\overline{\rho'^2}$ becomes definitely possible. A typical result is presented below.

Table I Run No. 4F Axial position 2.0" Radial position 0.2"

No. of calculations	$\frac{(\overline{\rho'^2})^{\frac{1}{2}}}{\bar{\rho}}$	$\frac{\overline{\rho' u'}}{(\overline{\rho'^2})^{\frac{1}{2}}\ (\overline{u'^2})^{\frac{1}{2}}}$	$\frac{(\overline{u'^2})^{\frac{1}{2}}}{\bar{U}}$
(1)*	0.23	- 1.01	0.215
(2)	0.2	- 0.86	0.217
(3)	0.4	- 0.771	0.221
(4)	0.5	- 0.74	0.226
(5)	0.6	- 0.736	0.232

*based on Equation V-2

From the above table, calculation number (1) shows that the values of 0.23 and 0.215 for

$$\frac{(\overline{\rho'^2})^{\frac{1}{2}}}{\bar{\rho}} \quad \text{and} \quad \frac{(\overline{u'^2})^{\frac{1}{2}}}{\bar{U}} ,$$

respectively, are very reasonable. However, the value of - 1.01 for

$$\frac{\overline{\rho' u'}}{(\overline{\rho'^2})^{\frac{1}{2}}\ (\overline{u'^2})^{\frac{1}{2}}}$$

is mathematically impossible as given by Cauchy's inequality,

$$-1 \leq \frac{\overline{\rho' u'}}{(\overline{\rho'^2})^{\frac{1}{2}} (\overline{u'^2})^{\frac{1}{2}}} \leq 1$$

Suspecting that $\overline{\rho'^2}$ as determined from the aspirator probe data is damped, the value of $\overline{\rho'^2}$ is steadily increased and results are given in calculations 2, 3, 4 and 5. In terms of percentages, when

$$\frac{(\overline{\rho'^2})^{\frac{1}{2}}}{\bar{\rho}}$$

is changed from 23% to 60%, $\frac{(\overline{u'^2})^{\frac{1}{2}}}{\bar{U}}$

changed from 21.5% to 23.2%. The correlation,

$$\frac{\overline{\rho' u'}}{(\overline{\rho'^2})^{\frac{1}{2}} (\overline{u'^2})^{\frac{1}{2}}} ,$$

which has an erroneous value initially, gradually assumes a more feasible value. This is a definite indication that the density fluctuation is damped.

It should also be noted that there exists a limit wherein the value of the density turbulent intensity

$$\frac{(\overline{\rho'^2})^{\frac{1}{2}}}{\bar{\rho}}$$

can not be exceeded. This comes from the fact that, unlike velocity, the density in the flow field can not be lower than that of air, 0.075 lb/ft^3, nor higher than that of Freon-12, 0.317 lb/ft^3. For instance, the

density at the point in which the quantities in Table I were calculated is 0.183. Hence, the maximum fluctuation which is the difference of 0.075 from 0.183 is .108. This fluctuation corresponds to a maximum density turbulence intensity of 0.59.

Another behavior that is worth noting is the seeming lack of dependence of $\overline{u'^2}$ on $\overline{\rho'^2}$ as can be observed in Table I. The reason for this behavior has been explained in the chapter on "Analytical Discussion."

Results for the turbulence intensities are shown in Figures V1-2, V1-3, V1-4 and V1-5. The profiles in Figures V1-2 and V1-3 show a maximum turbulence intensity of about 70% at 1.0" downstream. These maxima are close to the center line and are very different from the velocity and density profiles. At $\frac{1}{4}$" and $\frac{1}{2}$" downstream, the profile peak at about 50% at

$$r/r_0 \approx 0.84$$

These peaks are narrow initially and then gradually widens with the peak value falling off. At 2", the maximum is near 30%. They then become flatter, similar looking profiles at 4", 6" and 10" with the maxima at 15% to 8%. The free stream turbulence intensity is about 3%.

The turbulence intensity field could be divided into two main regions. An initial region, characterized by high narrow peaking of the profiles and a "similarity" region where profiles are apparently similar. The initial

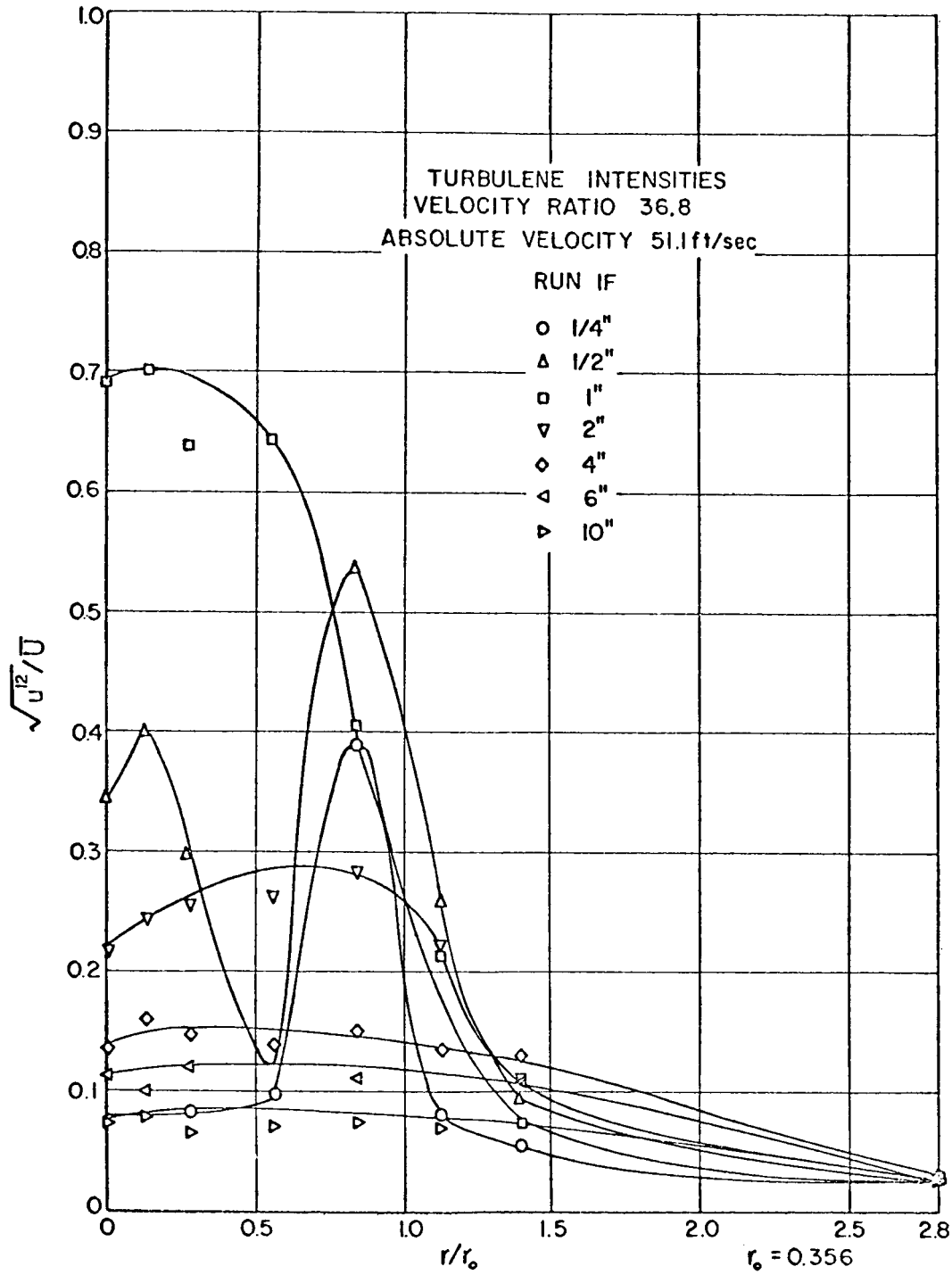

FIGURE VI - 2 TURBULENCE INTENSITY PROFILE

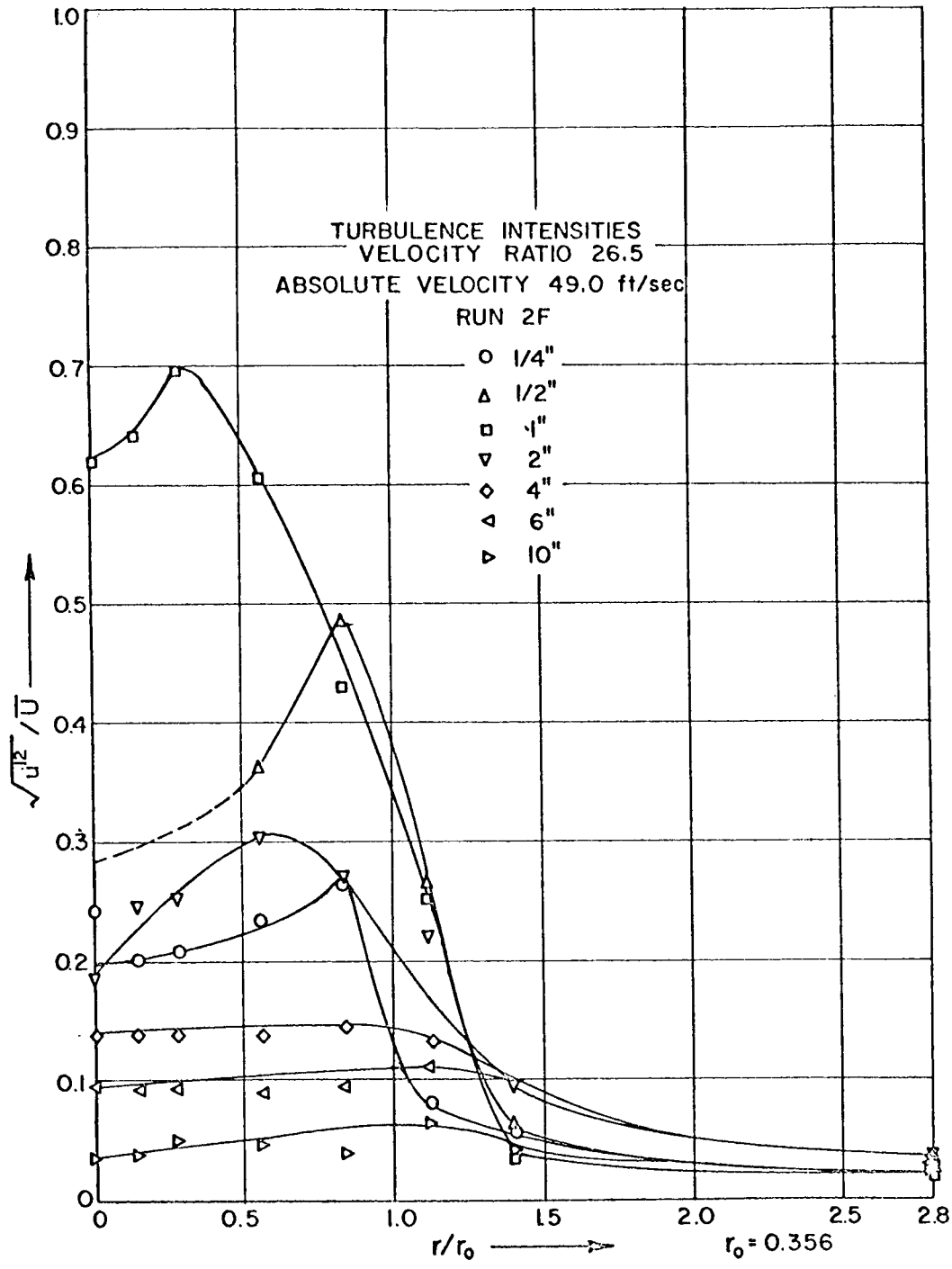

FIGURE V1 - 3 TURBULENCE INTENSITY PROFILE

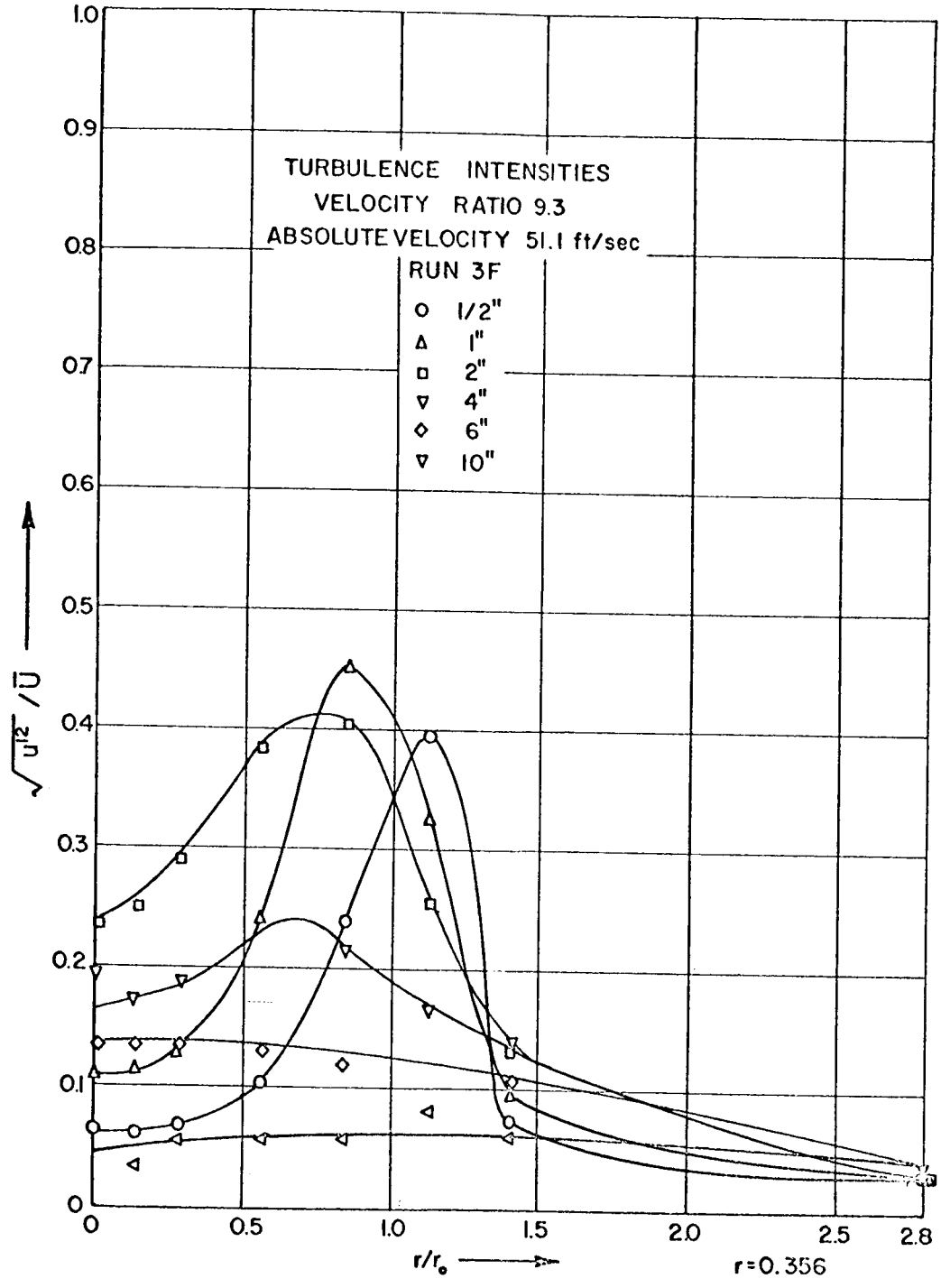

FIGURE V1 - 4 TURBULENCE INTNESITY PROFILE

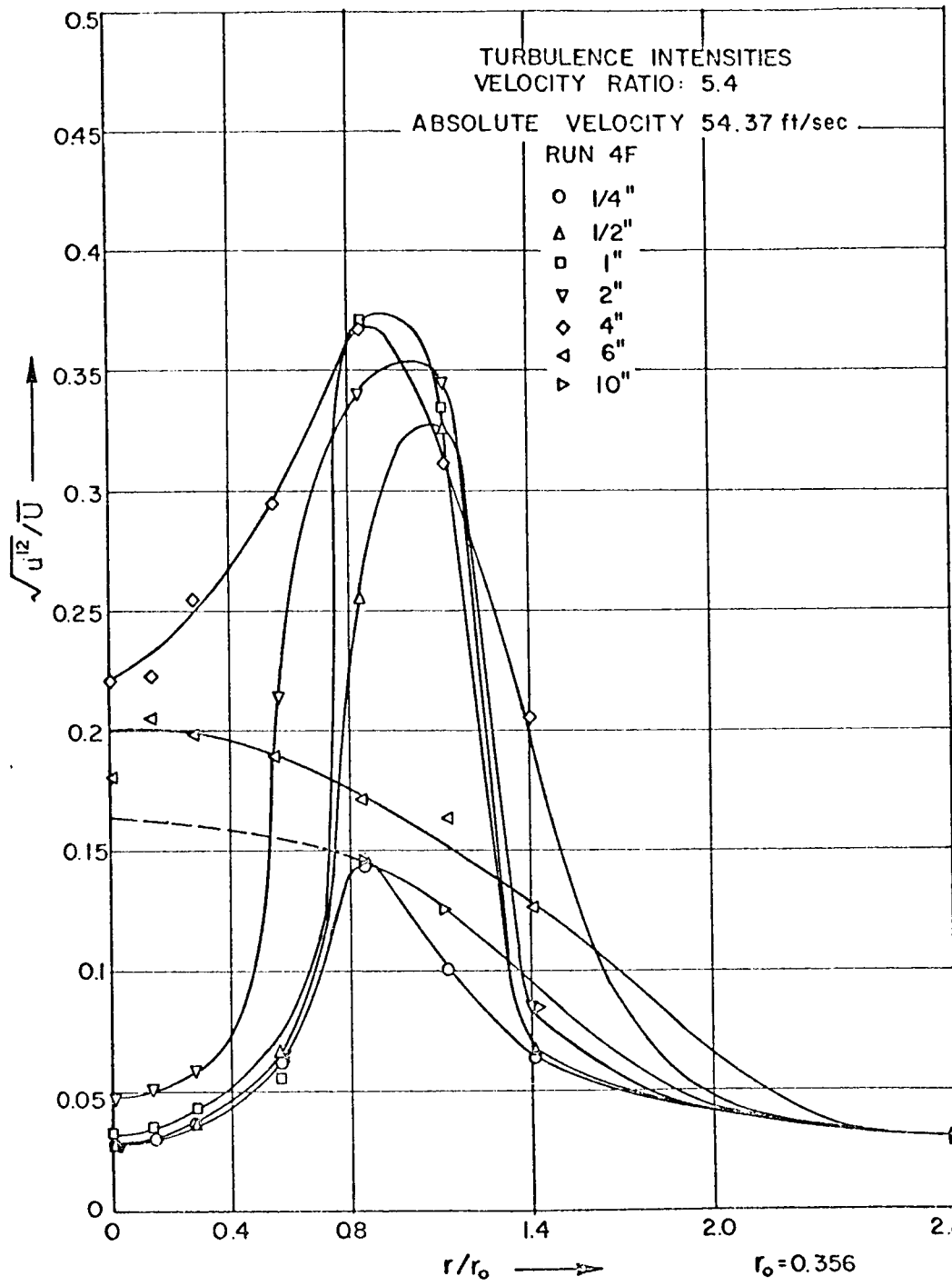

FIGURE VI - 5 TURBULENCE INTENSITY PROFILE

region is restricted to an axial position of 2.0" for the high velocity cases and extends from 4.0" to 6.0" at the lower velocity ratio cases.

In the region close to the jet opening, the data reported may not be very accurate. Because this is a region of low velocity, it is difficult to get satisfactory results.

B. Velocity Profiles

Figures V1-6, V1-7, V1-8 and V1-9 show typical velocity profiles taken at various velocity ratios. The effects of radial and axial momentum transfer by viscous force is very evident in all the curves.

In addition to viscous forces, inertia, pressure, bouyant forces, boundary effects, etc., affects the momentum of a particle in the flow field. Two peculiar observations that can be interpreted in terms of the actions of these forces are noted.

(1) At about four inches downstream, the centerline velocity is inversely proportional to the initial inner stream velocity, though intuition leads one to believe it to be directly proportional. If centerline velocity at various parts downstream is plotted against initial velocity, the curve is as shown in Figure V1-10. The behavior can be explained this way: At low initial velocity, the amount of fluid to be accelerated is less, hence viscous force can accelerate the fluid particles to a higher velocity

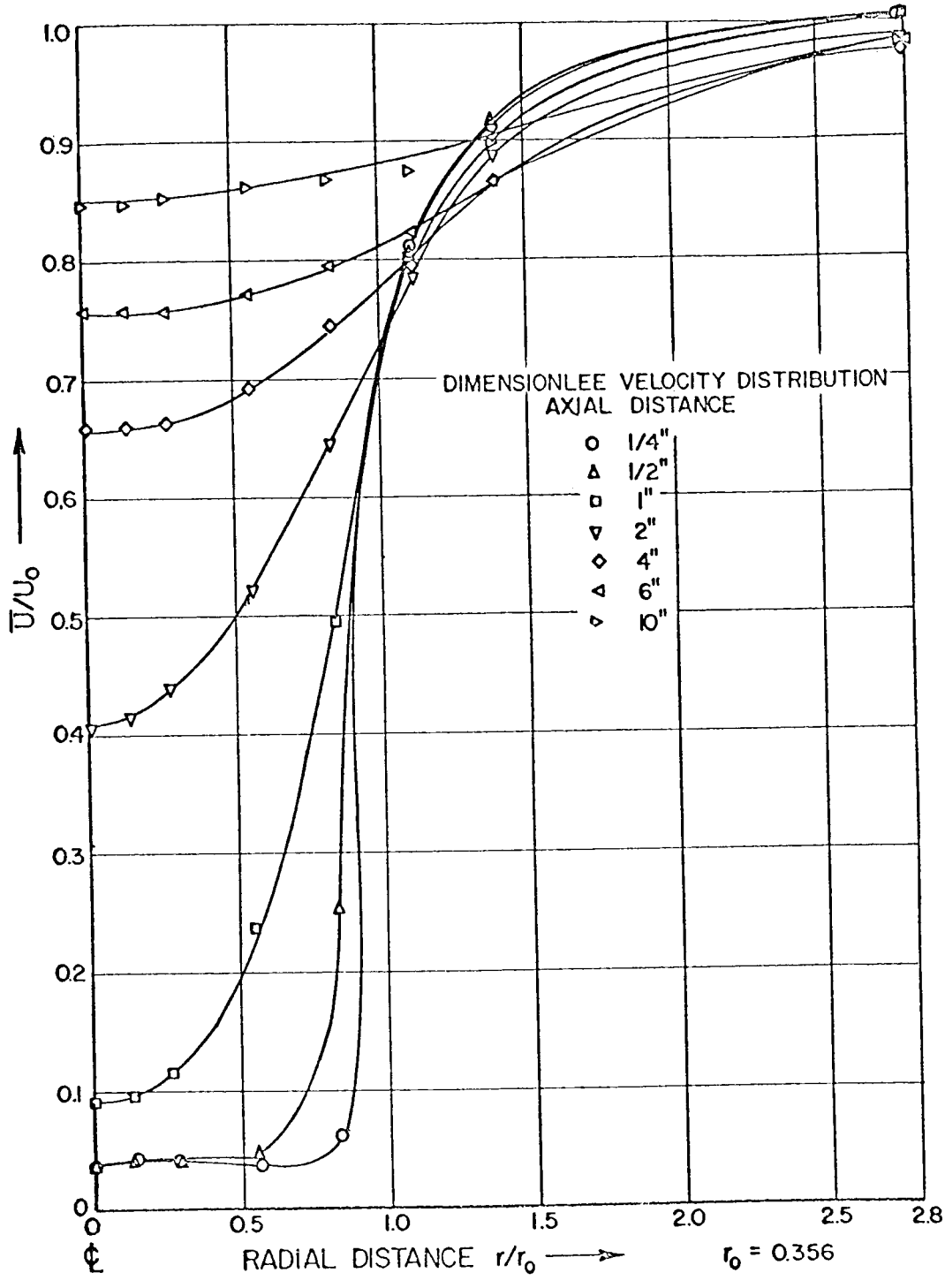

FIGURE VI - 6 DIMENSIONLESS VELOCITY PROFILE

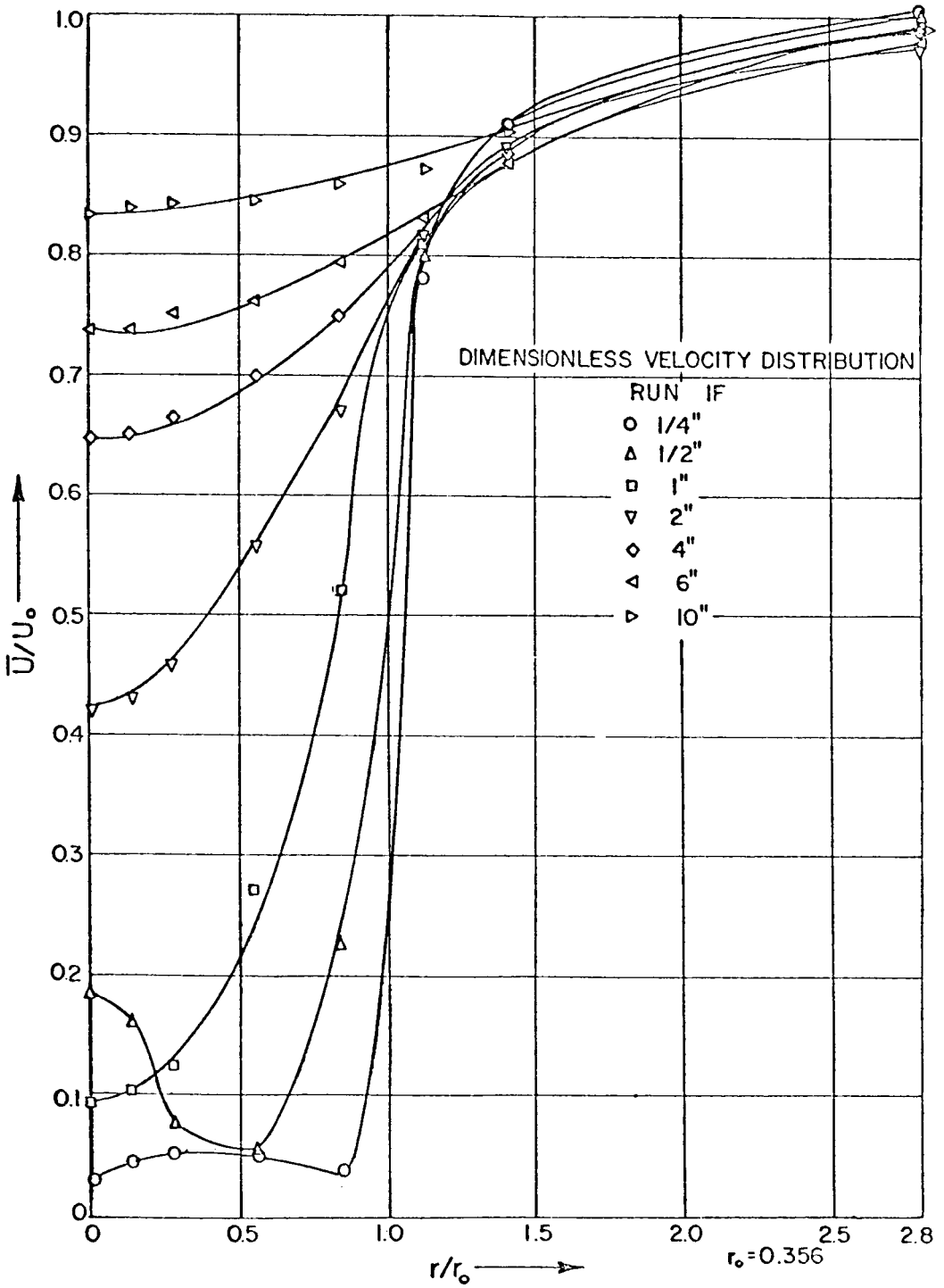

FIGURE VI - 7 DIMENSIONLESS VELOCITY PROFILE

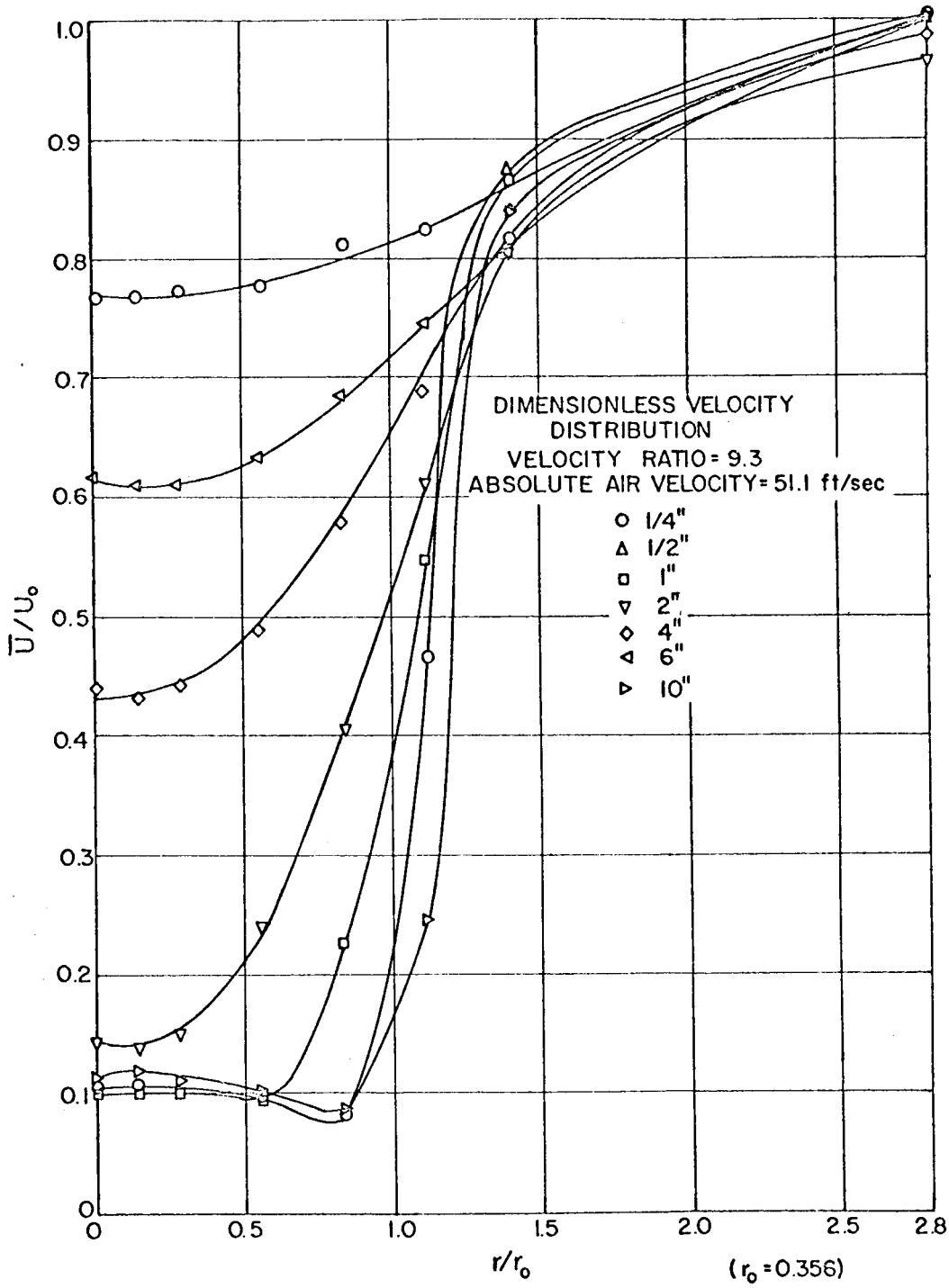

FIGURE VI - 8 DIMENSIONLESS VELOCITY PROFILE

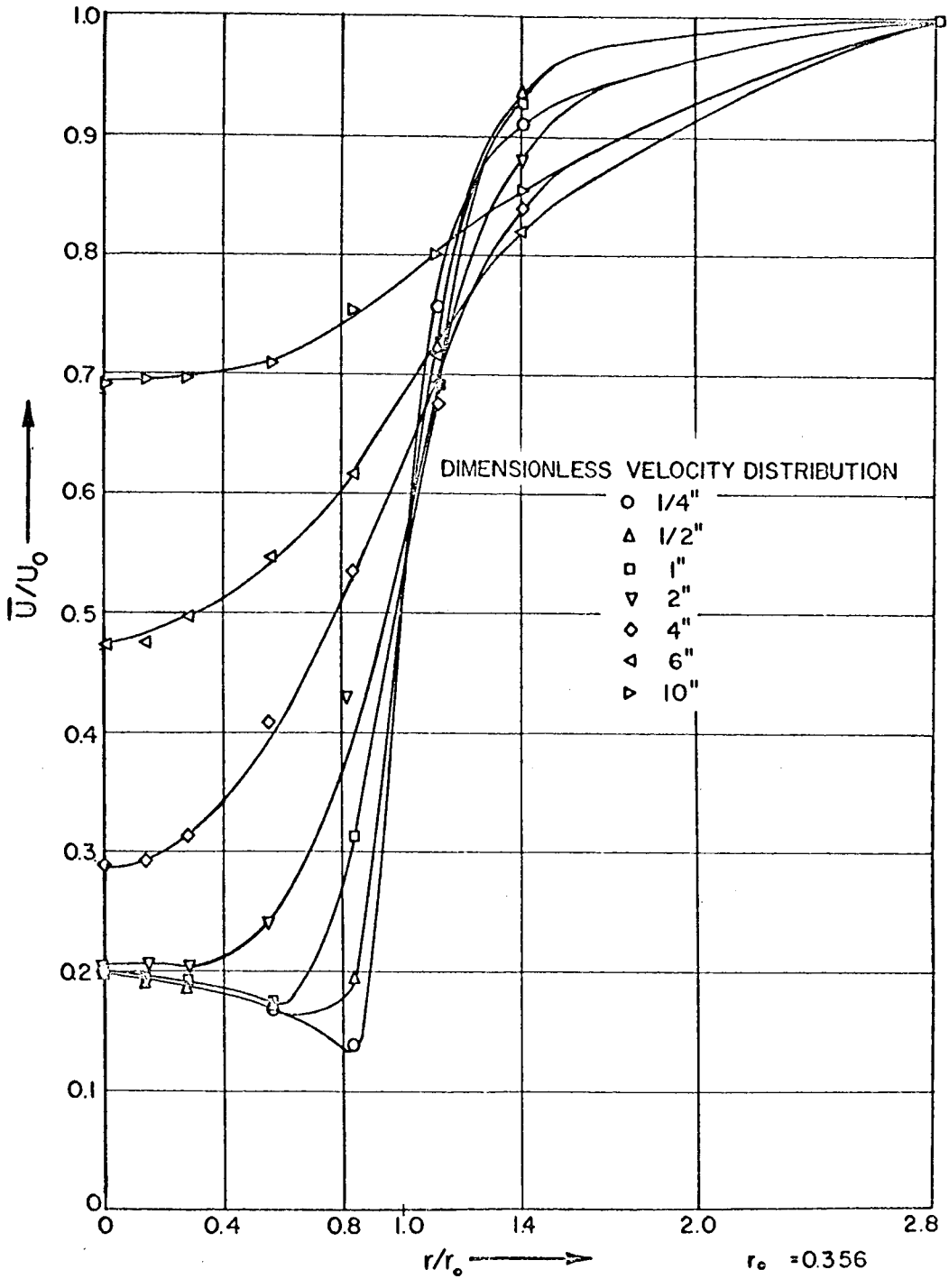

FIGURE VI - 9 DIMENSIONLESS VELOCITY PROFILE

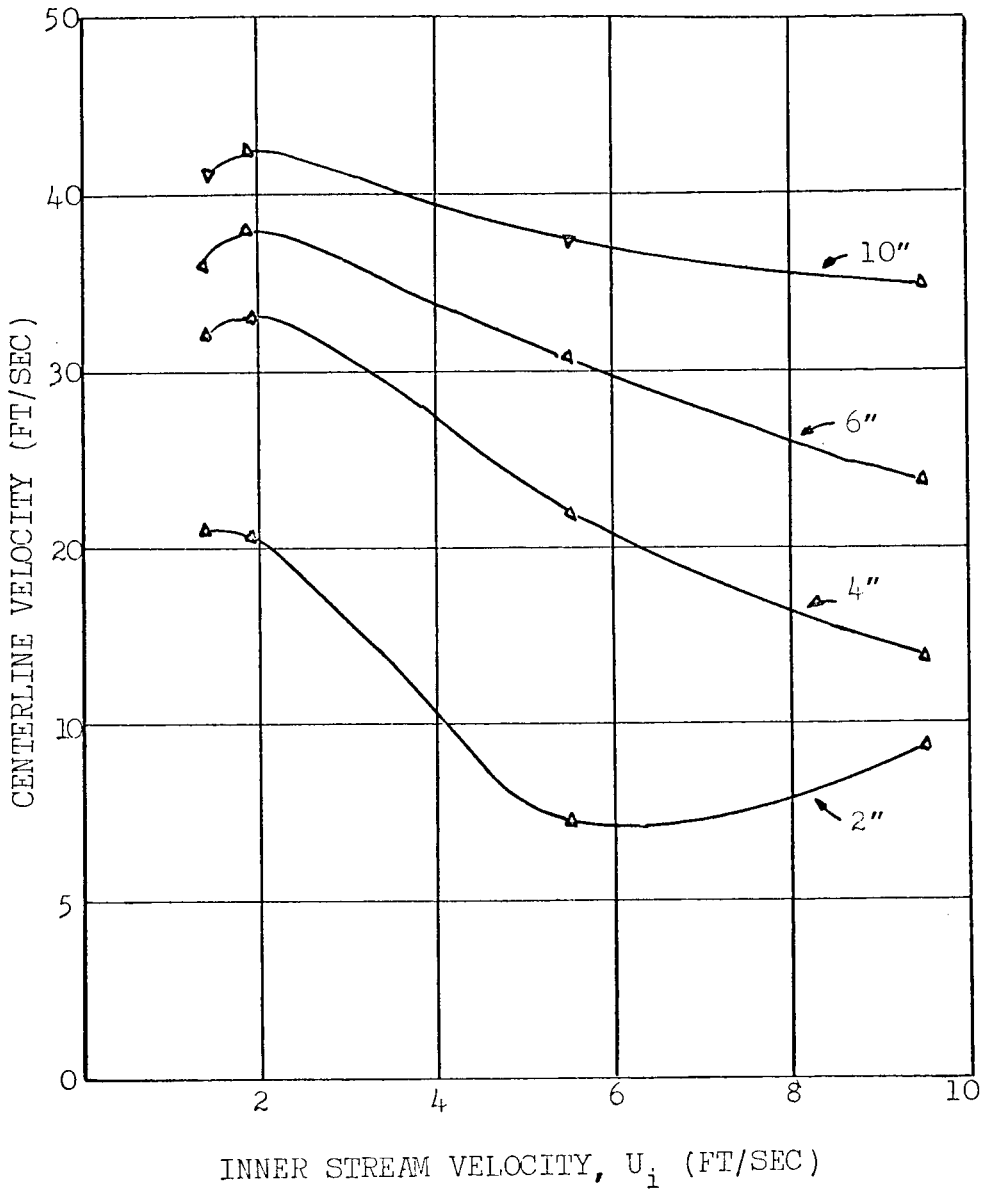

FIGURE VI-10 GRAPH OF CENTERLINE VELOCITY VERSUS INITIAL VELOCITY OF STREAM

at a shorter distance. The higher the initial flow rate, the longer the distance it will take to attain the outside air velocity. However, if we go on increasing the initial flow rate, it begins to approach the outer stream velocity. Obviously there will be a minimum in downstream velocity.

This explanation will be supported by the following simplified analysis.

The change in momentum (final minus initial momentum) required to attain a velocity, say U_o, by a stream in plug flow is given by

$$\Delta M = U_o(\rho A_t U_i) - U_i(\rho A_t U_i) =$$

$$\rho A_t U_i [U_o - U_i] \qquad \text{VI-1}$$

Where ρ is density, A_t is cross sectional area of tube, U_i is initial velocity, U_o is final velocity. Equation VI-1 shows that ΔM is small at low velocity because U_i is small, becomes gradually larger as U_i is increased, and then decreases again because $(U_o - U_i)$ becomes smaller. The velocity where ΔM is maximum is found by differentiating Equation VI-1, and is given below

$$U_i = \frac{U_o}{2} \qquad \text{VI-2}$$

A similar result is obtained for streams in laminar flow

$$\text{Initial momentum} = \int_0^R U_i^2 \, \rho \, 2 \, \pi \, r \, d \, r$$

Substituting the Hagen-Poiseuille relation for velocity in a pipe and integrating gives

$$M_i = 4 \rho A_t U_i^2 \qquad \text{VI-3}$$

Where M_i = initial momentum, A_t is tube cross-sectional area, U_i is average velocity in tube.

$$\text{final momentum} = U_o U_i \rho A_t$$

Hence,

$$\Delta M = \rho A_t U_i \left[U_o - \frac{4}{3} U_i\right] \qquad \text{VI-4}$$

and ΔM maximum occurs at

$$U_i = \frac{3}{4} U_o \qquad \text{VI-5}$$

Equations VI-4 and VI-5 show that there is an initial velocity in which the change in momentum required to accelerate a fluid stream of a given cross-sectional area to a given velocity U_o is a maximum. Consequently, there also exists a certain initial velocity in which the change in velocity required to effect a given change in momentum will be minimum.

For plug flow, this occurs at

$$U_i \text{ minimum} = \sqrt{\frac{\Delta M}{\rho A_t}} \qquad \text{VI-6}$$

For laminar flow

$$U_i \text{ minimum } = \sqrt{\frac{3\ \Delta M}{4\ \rho\ A_t}} \qquad \text{V1-7}$$

Equations V1-6 and V1-7 show that assuming equal accelarative forces are acting (Δ M), the fluid stream which has an initial velocity in the range

$$\left(\frac{3\ \Delta M}{4\ \rho A_t}\right)^{\frac{1}{2}} \leq U_i \leq \left(\frac{\Delta M}{\rho A_t}\right)^{\frac{1}{2}}$$

will attain the lowest velocity. The range in values of U_i follows from the fact that flow in turbulent pipes is midway between the two extremes, flat flow and laminar flow.

(2) The center line velocity from the mouth of the nozzle does not immediately increase, but decreases for the first 1/2" downstream, before starting to increase. This phenomenon has been observed only when the air-to-freon velocity ratio is high. Its presence is analagous to the existence of "backflow" behind the wake of a sphere or a cylinder. However, "backflow" in the system being discussed is manifested as a net reduction in velocity and is observed only at high velocity ratios.

C. Density Profile

Figures V1-11, V1-12, V1-13 and V1-14 are density profiles at various distances downstream. A comparison of the density

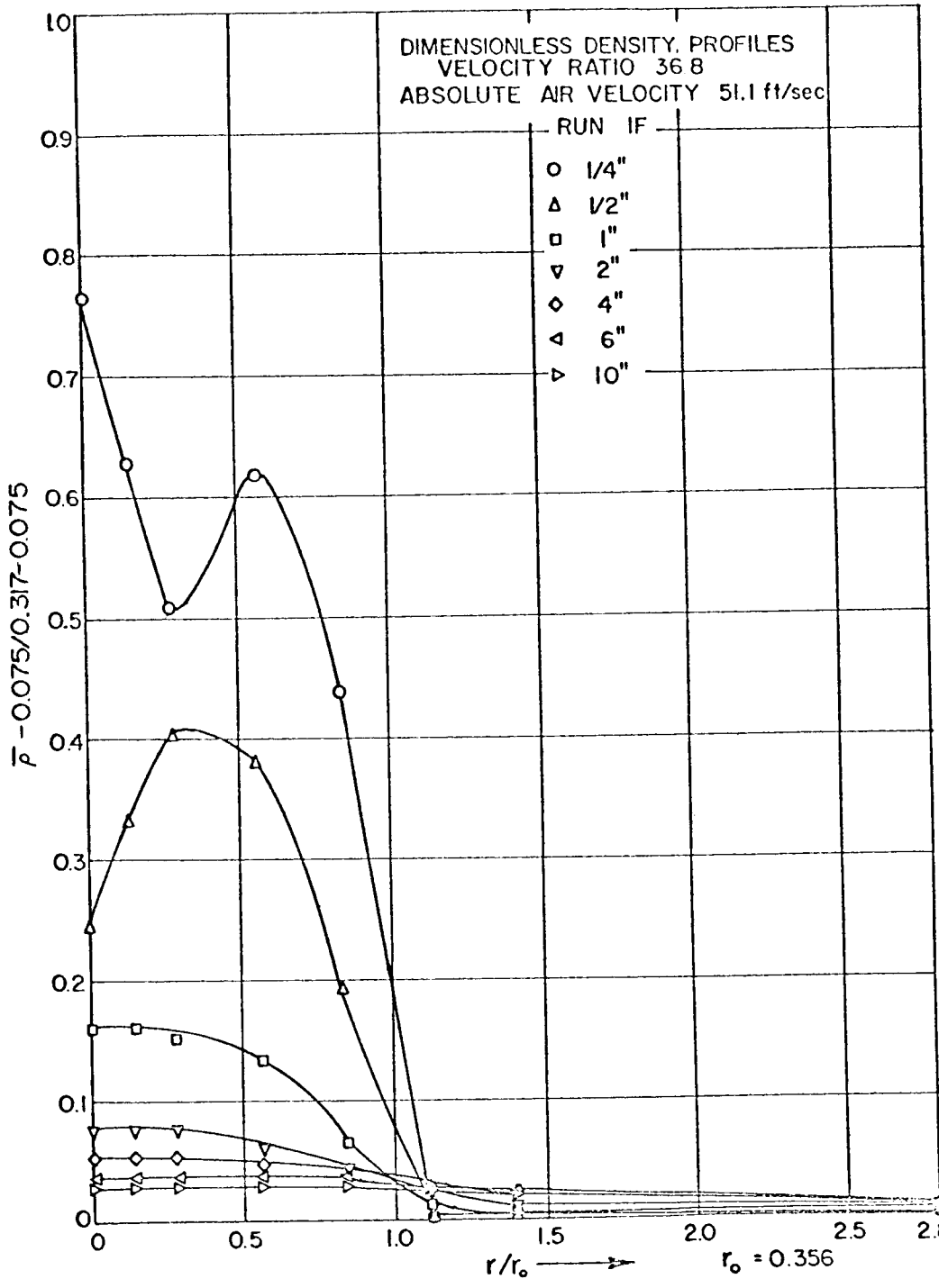

FIGURE VI - 11 DIMENSIONLESS DENSITY PROFILE

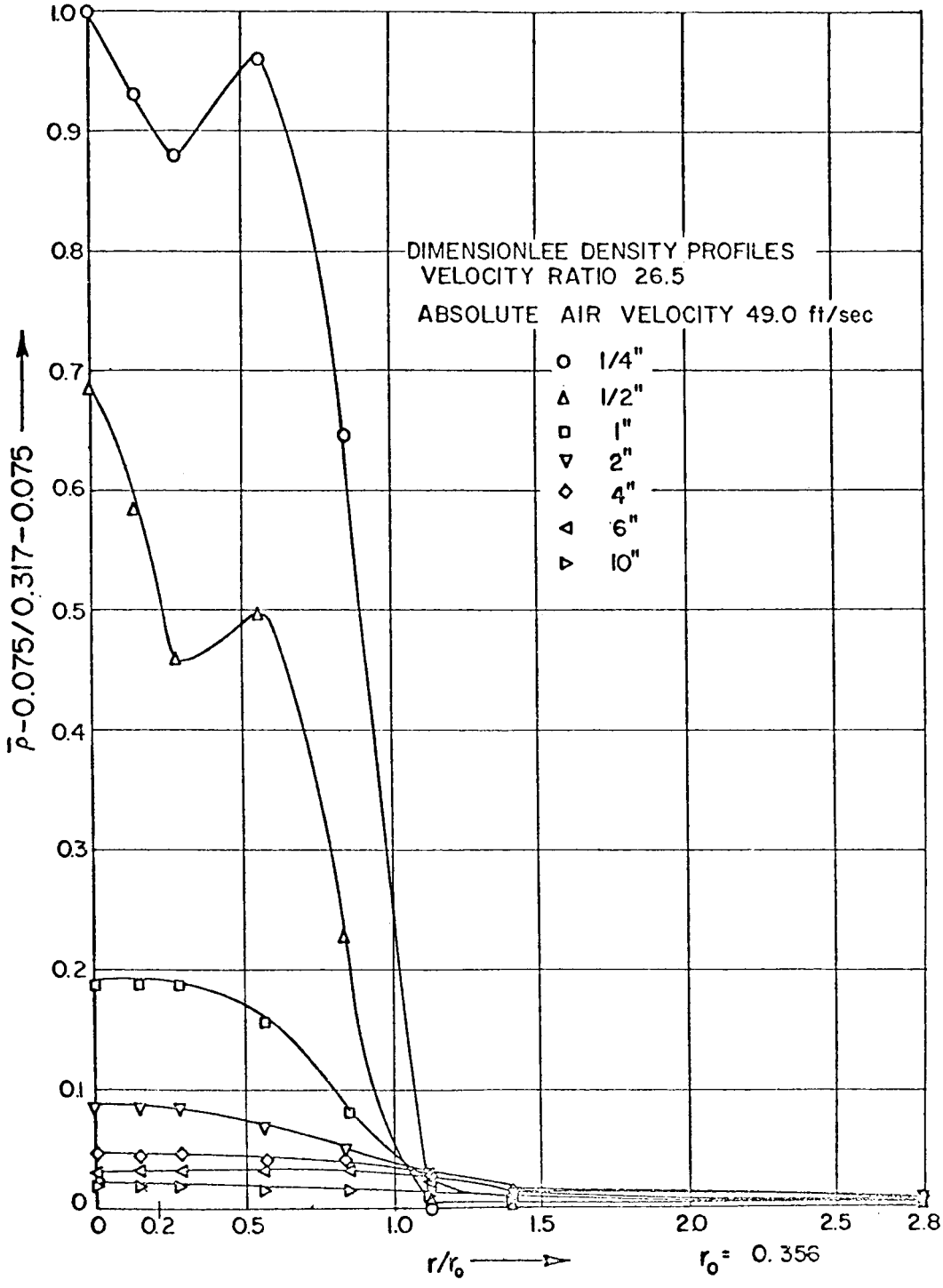

FIGURE VI - 12 DIMENSIONLESS DENSITY PROFILE

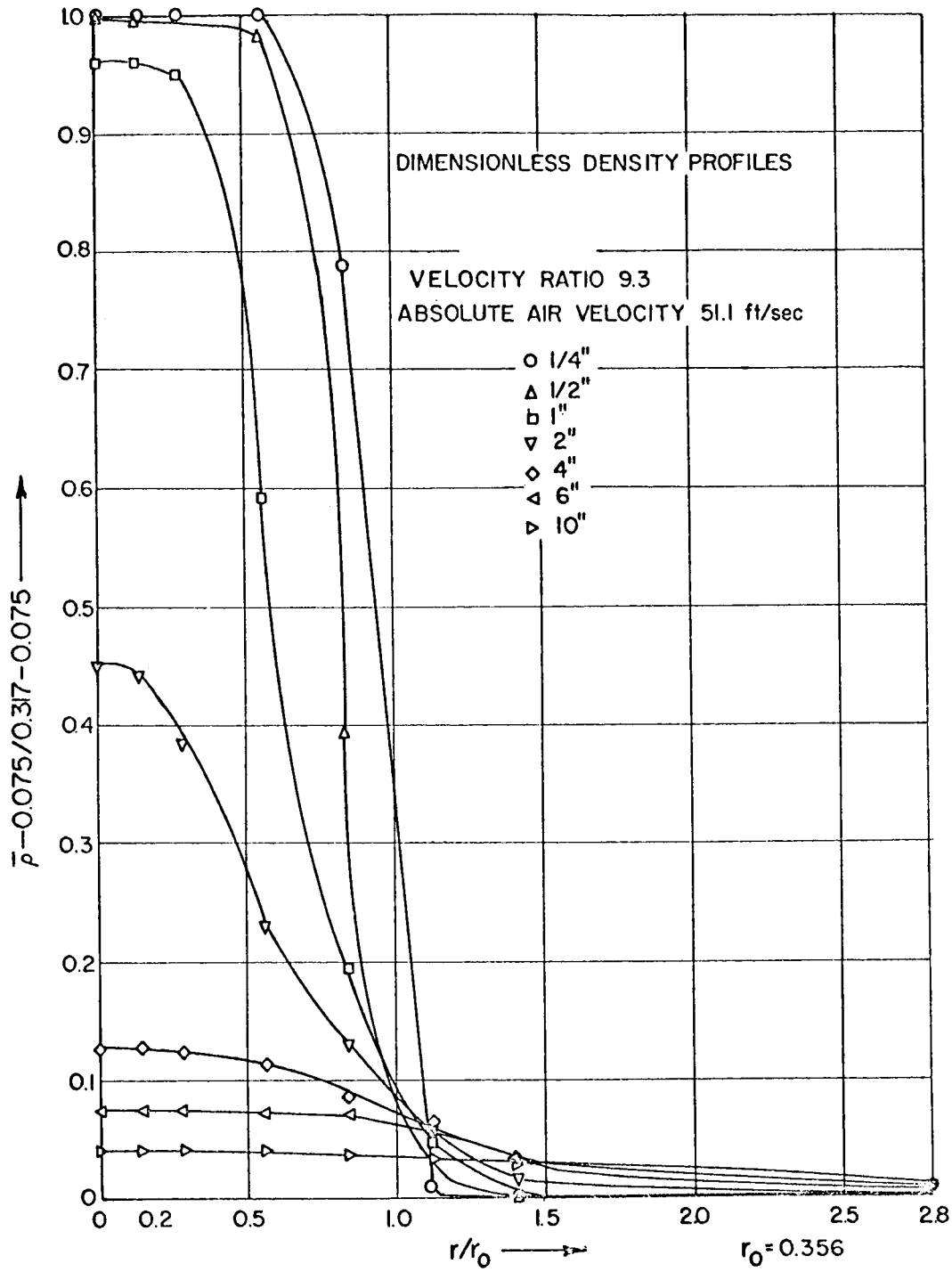

FIGURE VI - 13 DIMENSIONLESS DENSITY PROFILE

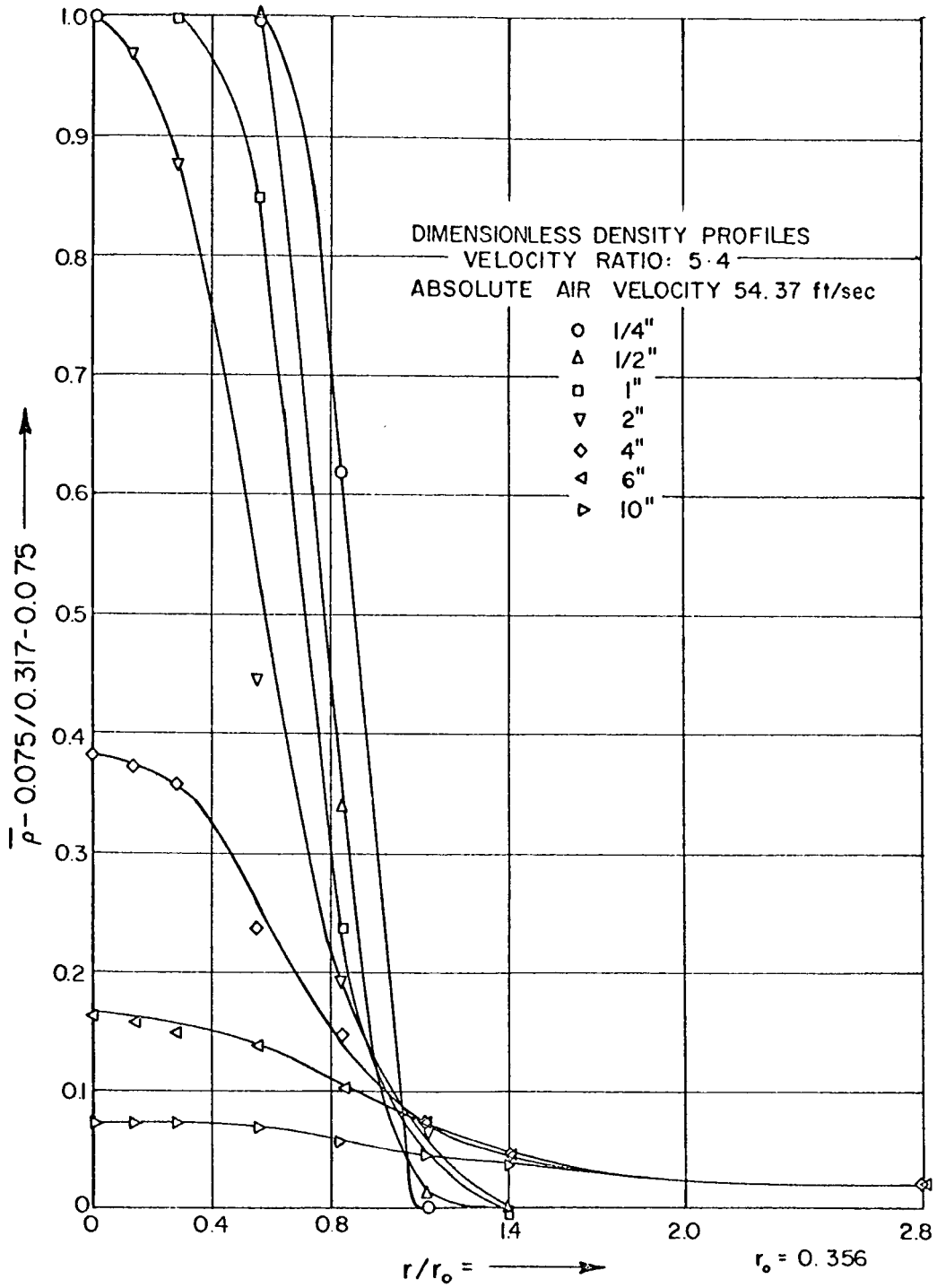

FIGURE VI · 14 DIMENSIONLESS DENSITY PROFILE

and velocity profiles shows that the density assumes a flat profile at a shorter axial distance than the velocity. In general, it can be said that the transfer of mass occurs at a faster rate than transfer of momentum.

It also appears that there are at least four regions of flow: (1) The small undisturbed core of Freon-12 which exists as far as 2" downstream (Figure VI-15) for a velocity ratio of 5.4. (2) A centrally located mixing zone where most of the mixing takes place. This region covers a cross sectional area the size of the pipe cross section, and it extends to a considerable distance downstream. (3) A middle section wherein concentration changes are negligible compared to the mixing zone. (4) Outer undisturbed outer stream. These regions in the flow stream are depicted in Figure VI-15.

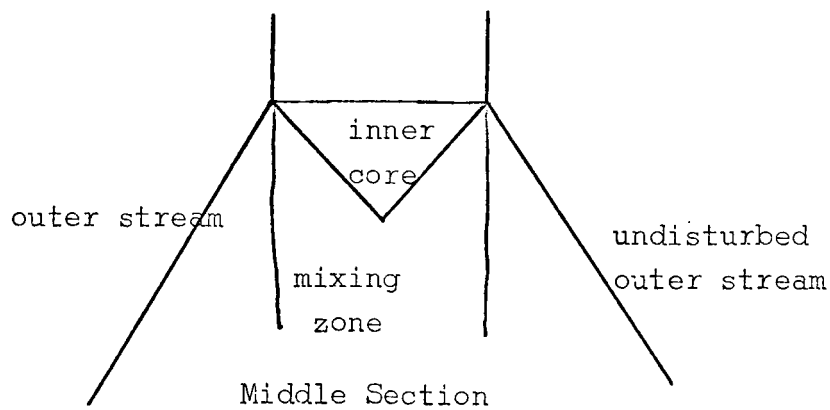

Figure VI-15 - Axial cross section of flow stream in coaxial flow showing the different density regions.

An interesting occurrence at the high velocity ratio (See Figures VI-11, 12, and 13) is the presence of a hump in the

density profile at 1/4 and 1/2 inch downstream of the initial face. The expected curve is one with a monotonic decrease of density as radial distance increases.

This might be explained in part by Equation V-1, which gives the relation of average power to density.

$$P_d(\bar{\rho}) = \bar{P}_d - \frac{d^2P_d}{d\rho^2}\overline{\rho'^2} - \frac{d^3P_d}{d\rho^3} - \ldots \qquad \text{V-1}$$

At large density fluctuations, the correction terms

$$- \frac{d^2P_d}{d\rho^2}\overline{\rho'^2} - \ldots$$

which give a positive error to the average power might not be negligible. For instance, for run 4F, axial position 2.0 and radial position 0.2",

$\bar{P}_d = 1.604$

$\overline{\rho'^2} = .001777$

$\frac{d^2P_d}{d\rho^2}$ is found by differentiating the power expression given in the sample calculation of Chapter V.

$$\frac{d^2P_d}{d\rho^2} = \frac{2 * 1.017}{.225^2} - \frac{6 * .396}{.225^2}\left(\frac{\rho - .075}{.225}\right) = 17.6$$

From Equation V-1

$$P_d(\bar{\rho}) = 1.604 - (.00177)(17.6) = 1.573$$

From Figure IV-3

$\bar{\rho} = 0.199$ which differs from .183 by 8.5%.

The net effect of neglecting these terms is that a lower density reading is obtained. The fact that the density fluctuation is highest when the measured density is lower than expected, partially supports this hypothesis. In the density profile curves, the spots where humps might occur are indicated in Figure VI-16

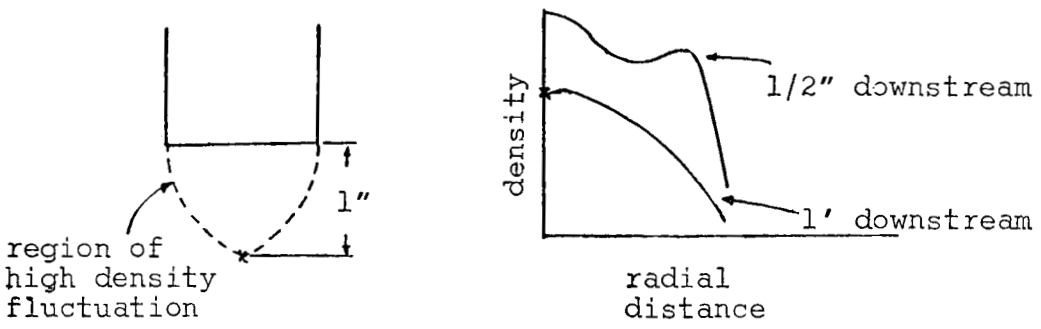

Figure VI-16 Regions where density profile might show humps

However, it was found that the magnitudes of the error corrections were much smaller than the deviations observed. A correction of about 10% in the density calculations brought the deviations to within 50% of their expected values. No other reason for the occurrence of the phenomenon can be given.

CONCLUSIONS

(1) It has been indicated in the literature that the power loss from three independent hot film anemometers can provide a means for determining

$$\overline{\rho'^2}\ , \quad \overline{\rho' u'}\ , \quad \text{and} \quad \overline{u'^2}$$

For the flow system considered, it was found that the magnitude of the experimental error in the data is as large as the value of $\overline{\rho'^2}$ and, hence, the equations are not really independent. Another method to estimate $\overline{\rho'^2}$ is necessary.

(2) The fluctuating power recorded by the aspirator probe is not a measure of the fluctuating density in the flow field but of that in the aspirator probe. These fluctuations are considerably damped from those in the free stream.

(3) Because of the relationship between $\overline{\rho'^2}$ and $\overline{u'^2}$ a large change in the magnitude of $\overline{\rho'^2}$ usually has only a small effect on the magnitude of $\overline{u'^2}$ at the range where the power loss equations are applicable.

(4) The turbulence intensity profiles may be divided into an initial region and a similar region, much like the density and velocity profiles.

(5) In the initial region, intensities are higher than in the similar portion with maxima having magnitudes of about 40%. In the similar region, maximum intensities are about 15%. The maximum depends on the velocity ratio of the streams.

BIBLIOGRAPHY

1. Schlichting, H., "Laminare Strahlausbreitung" ZAMM% 13, 1933.

2. Andrade, E.N., "The Velocity Distribution in a Liquid into Liquid Jet - The Plane Jet". Proc. Phys. Soc. Lond. 51, 1939.

3. Zawacki, T., Ph. D. Thesis "Turbulence in the Mixing Region of Co-axial Streams". Ill. Inst. of Tech. 1967.

4. Abramavitch, G.N., "The Theory of Turbulent Jets. M.I.T. Press. Cambridge, Mass. 1963.

5. Tollmien, W., "Berechnung Turbulenter Aus breitungsvorgange" ZAMM 6, 1926 Translated as NACA TM 1085, 1945.

6. Goertler, H., "Berechnung von Aufgaben der freien Turbulenz auf Grund eines neuen Naherungsansatzes" ZAMM 22, 1942.

7. Keuthe, A.M., "Investigation of the Turbulent Region Formed by Jets" Journal of Applied Mechanics, Trans. ASME Vol. 57, 1935.

8. Squire, H.B. and Trouncer, J., "Round Jets in a General Stream" Aeronautical Research Committee Technical Report, R and M No. 1974, 1944.

9. Ferri, A., Libby, P.A. and Zakkay, V., "Theoretical and Experimental Investigations of Supersonic Combustion" Aeronautical Res. Lab. Report ARL 62-467 Sept. 1962.

10. Alpinieri, L.J., "An Experimental Investigation of the Turbulent Mixing of Non-homogeneous Co-axial Jets". Polytech. Inst. of Brooklyn, Pibal Rept. 689, 1963, also "Turbulent Mixing of Co-axial Jets AIAA. Journal Vol. 2 1964.

11. Ragsdale, R.G., Weinstein, H. and Lanzo, C.D., "Correlation of a Turbulent Air-Bromine Co-axial Flow Experiment".

12. Boehman, L., "Mass and Momentum Transport Properties in Isoenergetic Co-axial Flows", Ph.D. Thesis, Illinois Inst. of Tech. 1966.

13. Weinstein, H. and Todd, C.A., "Analysis of Mixing of Co-axial Streams of Dissimilar Fluids Including Energy Generation Terms.

14. Corrsin, S., Natl. Advisory Committee Aeronaut. Wartime Reports No. 94, 1943.

15. Corrsin, S., and Uberoi, M.S., "Further Experiments in the Flow and Heat Transfer in a Heated Turbulent Jet" NACA Rept. 998, 1950.

16. Tani, I. and Kobashi, Y., "Experimental Studies on Compound Jets" Proceedings of the 1st Japan National Congress for Appl. Mech., 1951.

17. Kobashi, Y., "Experimental Studies on Compound Jets" (measurement of turbulent characteristics) Proceedings of the 2nd Japan National Congress for Appl. Mech. 1952.

18. Rosensweig, R.E., "Measurement and Characterization of Turbulent Mixing Fuels" Res. Lab. May, 1959.

19. Blackshear, Jr., P.L. and Fingerson, L., "Rapid Response Heat Flux Probe for High Temperature Gases", ARS Journal, Nov. 1962.

20. Conger, W.L., "Measurement of Concentration Fluctuations in the Mixing of Two Gases by Hot-wire Anemometer Techniques". Ph.D. Thesis Univ. of Penn. 1965.

21. King, L.V., Phil Trans Roy. Soc. London 214A pg. 273, 1917.

22. Van der Hegge Zijnen, B.G., Appl. Sci. Research 6A pg. 129, 1956.

23. Kramers, H., Physica 12, pg. 61, 1946.

24. Corrsin, S., "Extended Applications of the Hot Wire Anemometer" NACA Technical Note 1864, 1949.

25. D'Souza, G.J., M.S. Thesis, "Turbulence Correlations in a Co-axial Flow of Dissimilar Fluids", Illinois Inst. of Tech. 1967.

26. Hinze, J.O., "Turbulence" McGraw-Hill Book Co.

"The aeronautical and space activities of the United States shall be conducted so as to contribute . . . to the expansion of human knowledge of phenomena in the atmosphere and space. The Administration shall provide for the widest practicable and appropriate dissemination of information concerning its activities and the results thereof."

—NATIONAL AERONAUTICS AND SPACE ACT OF 1958

NASA SCIENTIFIC AND TECHNICAL PUBLICATIONS

TECHNICAL REPORTS: Scientific and technical information considered important, complete, and a lasting contribution to existing knowledge.

TECHNICAL NOTES: Information less broad in scope but nevertheless of importance as a contribution to existing knowledge.

TECHNICAL MEMORANDUMS: Information receiving limited distribution because of preliminary data, security classification, or other reasons.

CONTRACTOR REPORTS: Scientific and technical information generated under a NASA contract or grant and considered an important contribution to existing knowledge.

TECHNICAL TRANSLATIONS: Information published in a foreign language considered to merit NASA distribution in English.

SPECIAL PUBLICATIONS: Information derived from or of value to NASA activities. Publications include conference proceedings, monographs, data compilations, handbooks, sourcebooks, and special bibliographies.

TECHNOLOGY UTILIZATION PUBLICATIONS: Information on technology used by NASA that may be of particular interest in commercial and other non-aerospace applications. Publications include Tech Briefs, Technology Utilization Reports and Notes, and Technology Surveys.

Details on the availability of these publications may be obtained from:

SCIENTIFIC AND TECHNICAL INFORMATION DIVISION

NATIONAL AERONAUTICS AND SPACE ADMINISTRATION

Washington, D.C. 20546